Petri Ahonen

Aerosol production and crystallization of titanium dioxide from metal alkoxide droplets

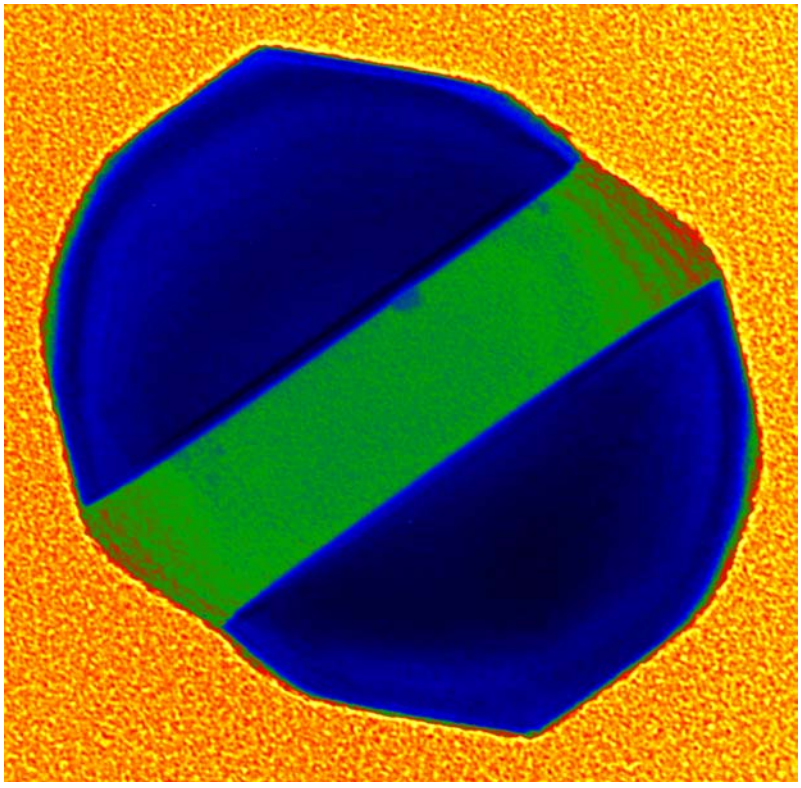

TECHNICAL RESEARCH CENTRE OF FINLAND ESPOO 2001

VTT PUBLICATIONS 439

Aerosol production and crystallization of titanium dioxide from metal alkoxide droplets

Petri Ahonen

VTT Chemical Technology

Dissertation for the degree of Doctor of Science in Technology to be presented, with due permission for public examination and debate in Auditorium E at Helsinki University of Technology (Espoo, Finland) on the 14th of September, 2001, at 13 o'clock.

TECHNICAL RESEARCH CENTRE OF FINLAND
ESPOO 2001

ISBN 951–38–5857–X (soft back ed.)
ISSN 1235–0621 (soft back ed.)

ISBN 951–38–5858–8 (URL:http://www.inf.vtt.fi/pdf/)
ISSN 1455–0849 (URL:http://www.inf.vtt.fi/pdf/)

JULKAISIJA – UTGIVARE – PUBLISHER

Valtion teknillinen tutkimuskeskus (VTT), Vuorimiehentie 5, PL 2000, 02044 VTT
puh. vaihde (09) 4561, faksi (09) 456 4374

Statens tekniska forskningscentral (VTT), Bergsmansvägen 5, PB 2000, 02044 VTT
tel. växel (09) 4561, fax (09) 456 4374

Technical Research Centre of Finland (VTT), Vuorimiehentie 5, P.O.Box 2000, FIN–02044 VTT, Finland
phone internat. + 358 9 4561, fax + 358 9 456 4374

VTT Kemiantekniikka, Prosessit ja Ympäristö, Biologinkuja 7, PL 1401, 02044 VTT
puh. vaihde (09) 4561, faksi (09) 456 7026, (09) 456 7021

VTT Kemiteknik, Prosesser och miljö, Biologgränden 7, PB 1401, 02044 VTT
tel. växel (09) 4561, fax (09) 456 7026, (09) 456 7021

VTT Chemical Technology, Processes and Environment,
Biologinkuja 7, P.O.Box 1401, FIN–02044 VTT, Finland
phone internat. + 358 9 4561, fax + 358 9 456 7026, + 358 9 456 7021

Cover picture:
A twinned rutile particle of 60 nm diameter which has been produced by titanium alkoxide droplet decomposition in an aerosol reactor at 1500°C (TEM image by Unto Tapper, VTT Chemical Technology, Finland).

Technical editing Leena Ukskoski

Otamedia Oy, Espoo 2001

Ahonen, Petri. Aerosol production and crystallization of titanium dioxide from metal alkoxide droplets. Espoo 2001. Technical Research Centre of Finland, VTT Publications 439. 55 p. + app. 62 p.

Keywords aerosols, particles, synthesis, pyrolysis, hydrolysis, alkoxides, titanium dioxide, anatase, rutile, crystal morphology

Abstract

In this experimental study, aerosol methods for producing titanium dioxide powders and increasing our knowledge of particle and crystal formation have been developed. Powders and ultrafine particles of titanium oxide were produced by an aerosol droplet decomposition route in tubular laminar flow reactors in air and nitrogen atmospheres. Reactor temperatures up to 1500°C were used with residence times in the range of 1–50 s. Novel methods were introduced for the production of micron sized powders, investigation of crystallization of anatase in the particles, and for studying the formation of crystal phase and morphology on ultrafine particles at different temperatures. High-resolution transmission electron microscopy, scanning electron microscopy, aerosol measurements by differential mobility analyzer and inertial impactor as well as materials characterization by diffraction and spectroscopic methods were performed. In addition, the production conditions in aerosol reactors were evaluated using computational fluid dynamics calculations. The results showed that titanium dioxide powders can be produced from ultrafine up to micron sized particles via droplet decomposition and in-droplet hydrolysis methods starting from a titanium alkoxide precursor. Crystal phase and crystallite size can be controlled by reactor conditions and by thermal post-annealing. Anatase formation in amorphous particles was observed near surfaces. Investigation of ultrafine particles revealed morphology development of rutile and anatase single crystals. The 60 and 120 nm diameter rutile crystal morphologies development was observed in mobility particle size measurements. The 20 nm diameter anatase particle morphology showed the development of crystallographic {011} and {001} surfaces.

Preface

The research work for this thesis was performed mainly in the Aerosol Technology Group, VTT Chemical Technology, Finland during 1997–2000. I wish to express my gratitude to my supervisor, Professor Esko Kauppinen, for his guidance and for providing excellent research facilities in aerosol and materials studies. The reactor experiments for Papers I and II were carried out in LMGP/ENSPG, Grenoble, France in 1997. I thank my supervisor of that time, Professor Jean-Claude Joubert, for providing guidance and facilities. Professor Pekka Hautojärvi is acknowledged for supervision of my PhD studies and guidance during writing of the thesis. I thank Professor Markku Leskelä and Professor Jorma Keskinen for their comments and suggestions of the thesis.

With pleasure I acknowledge my many collaborators in this work. Jorma Joutsensaari and Anna Moisala have collaborated in the experimental work. Unto Tapper, Olivier Richard and Gustaaf Van Tendeloo have supplied the study with excellent TEM analyses. David Brown and Jorma Jokiniemi have shared their computational modeling expertise. Jean-Luc Deschanvres performed Raman- and IR-spectroscopic analyses as well as provided much guidance during the months in France. Raoul Järvinen has helped in building experimental set-ups. I thank all my colleagues in the Aerosol Technology Group for a pleasant and helpful atmosphere.

This research work was funded by the National Technology Agency (Tekes) and VTT Chemical Technology. Personal support from the European Science Foundation via the NANO-program, and from Kemira Säätiö is gratefully acknowledged.

Cheerful greetings and thanks to my family, Anna, Lauri, Ville-Veikko, and Aaro as well as to my relatives and friends for their support.

Nummi-Pusula, May 2001

Petri Ahonen

List of publications

This thesis is based on the following publications. In the text they are referred to by Roman numerals.

I P. P. Ahonen, E. I. Kauppinen, J.-C. Joubert, J.-L. Deschanvres and G. Van Tendeloo. 1999. Preparation of nanocrystalline titania powder via aerosol pyrolysis of titanium tetrabutoxide. Journal of Materials Research, Vol. 14, pp. 3938–3948.

II P. P. Ahonen, U. Tapper, E. I. Kauppinen, J.-C. Joubert and J.-L. Deschanvres. 2001. Aerosol synthesis of Ti-O powders via in-droplet hydrolysis of titanium alkoxide. Materials Science and Engineering: A, Vol. 315, pp. 113–121.

III P. P. Ahonen, O. Richard and E. I. Kauppinen. 2001. Particle production and anatase formation in amorphous particles at in-droplet hydrolysis of titanium alkoxide. Materials Research Bulletin, Vol. 36, pp. 2017–2025.

IV P. P. Ahonen, J. Joutsensaari, O. Richard, U. Tapper, D. P. Brown, J. K. Jokiniemi and E. I. Kauppinen. 2001. Mobility Size Development and the Crystallization Path during Aerosol Decomposition Synthesis of TiO2 Particles. Journal of Aerosol Science, Vol. 32, pp. 615–630.

V P. P. Ahonen, A. Moisala, U. Tapper, D. P. Brown, J. K. Jokiniemi and E. I. Kauppinen. 2001. Gas-phase crystallization of titanium dioxide nanoparticles. Journal of Nanoparticle Research, submitted for publication.

Author's contribution

The author has had an active role in the research work reported in this thesis. He has strongly participated in planning the experiments and has performed all the experiments. The author has carried out most of the experimental data analysis and interpretation of the results. He has written the publications I–V.

The supervisor of the research work was Prof. Esko Kauppinen. In Papers I and II, Dr. Jean-Luc Deschanvres carried out the infrared- and Raman spectroscopy as well as supplying guidance in experimental planning and analysis. Prof. Gustaaf Van Tendeloo carried out the TEM analysis in Paper I, and Dr. Unto Tapper in Paper II. Both of the Paper I and II studies were performed under the additional supervision of Prof. Jean-Claude Joubert. In Paper III, Dr. Olivier Richard carried out the TEM analysis. In Papers IV and V, the experiments were accomplished with the help of Dr. Jorma Joutsensaari and Ms. Anna Moisala. The TEM analyses were performed by Dr. Tapper and Dr. Richard, and the computational fluid dynamics calculations by Dr. David Brown. Additional supervision was given by Dr. Jorma Jokiniemi.

Contents

Appendices of this publication are not included in the PDF version. Please order the printed version to get the complete publication (http://otatrip.hut.fi/vtt/jure/index.html)

List of symbols and acronyms

$C(D)$	slip correction factor
D_g	geometric mean diameters
D_{me}	mobility equivalent diameter
D_{ve}	volume equivalent diameter
l	reactor heated length
σ_g	geometric standard deviation
κ	dynamic shape factor
κ^o	continuum regime dynamic shape factor

BLPI	Berner type low pressure impactor
CFD	computational fluid dynamics
DMA	differential mobility analyzer
ED	electron diffraction
HR-	high resolution (TEM image)
ID	(reactor) inner diameter
NSD	number size distribution
SAD	selected area diffraction
SEM	scanning electron microscope
SSA	specific surface area
TEM	transmission electron microscope
TGA	thermogravimetric analysis
TTIP	titanium tetraisopropoxide
TTNB	titanium tetra-n-butoxide
XRD	X-ray diffraction
XRF	X-ray fluorescence

1. Introduction

Titanium dioxide is one of the most utilized particulate materials in the world. Although it was discovered more than 200 years ago and has been commercially processed for 85 years, it is still being actively researched. Pigmentary applications that are based on high refractive index, inertness, and negligible color, are by far the most common functions with a high tonnage of production. Recently, the production of ultraviolet active pigmentary material has been growing. Also, a number of other than pigmentary applications have come up. Many of them are based on the photocatalytic and semiconducting properties of titanium dioxide, *e.g.* the removal of organic impurities by oxidation as well as utilization in solar cells and self-cleaning paints. Particle size is important in these applications. Pigmentary properties are directly affected by the scattering unit dimension, and a high specific surface area, *i.e.* small crystallite size, is often desired in other applications. Therefore, aerosol production routes with well-controlled product particle size are advantageous. (Blakey & Hall 1988, Kroschwitz & Howe-Grant 1997)

A gas-phase route for production of titanium dioxide particles by oxidation of gaseous titanium tetrachloride (a continuous chloride process) was introduced in the late 1950's (Suyama & Kato 1976). Since then only a few other precursors have been introduced for aerosol production of titanium dioxide, of which titanium alkoxides are the most common. Production of titanium dioxide particles starting from precursor droplets was introduced in the late 70s when titanium propoxide and chloride droplets were hydrolyzed with water vapor in a flow reactor (Visca & Matijevic 1979). Pyrolysis of precursor droplets without water addition is the other route for droplet-to-particle processing although chemically not far from hydrolysis. While the chloride process is well established, the other aerosol routes and chemistries are far less studied. However, advanced aerosol methods can bring new insight into the area of titanium dioxide production, new well-controlled production methods, energy efficient production, and better properties.

While particle size is important in applications, the crystal structure of titanium dioxide must also be well controlled. Of several possible polymorphs, rutile and anatase are commercially produced for different functions, and the phase transformation between them is studied extensively. However, a general model

of crystal phase formation still seems to be lacking. Chemical recipes for preparation of different properties, *e.g.* in aerosol processed particles, can however easily be found in the literature. Microstructural characterization during phase transformation can be seen as an important tool for development from the present status of knowledge. In particular, combined with aerosol processing of nanostructured materials it can bring new perspectives and applications. (Penn & Banfield 1999, Joutsensaari 1999, Kodas & Hampden-Smith 1999)

The objectives of this study are to develop methods for producing titanium dioxide powders and further our knowledge of particle and crystal formation. In order to improve the properties of various products the production methods and properties still need to be studied. Knowledge of particle production and crystallization, on the other hand, is fundamental in controlling microstructure and, thus, the material properties. The production of titanium dioxide powders is technologically interesting and, in this thesis, aerosol systems for producing titanium dioxide powders have been studied.

This thesis is based on the publications I–V which are attached as appendices. The publications I, II and III present routes for producing titanium dioxide particles starting from a titanium alkoxide precursor. The pyrolysis of titanium butoxide droplets generated powder particles that were crystalline as processed or after a thermal treatment. An oxygen-deficient structure attained caused thermally stable anatase to be obtained. The other route, in-droplet hydrolysis, is a novel method for producing titanium dioxide powders. Further, the anatase crystallization in amorphous particle *in-situ* in reactor was investigated and was indicated as being initiated on the particle surface. In the publications IV and V, ultrafine particle formation as well as crystallization were studied. The experiments showed that rutile crystal morphology that was formed affected the particle mobility size. Crystal morphology developing in an anatase single crystal showed very distinctive crystallographic surfaces forming. The thesis is brought to a conclusion with a few suggestions for future studies.

2. Literature review

2.1 Titanium dioxide properties and crystal structure

Titanium dioxide (TiO_2) is a crystalline material with seven reported polymorphs, from which four are natural and others synthetic. Of the four natural polymorphs, rutile, anatase and brookite are commonly encountered in inorganic syntheses. Only rutile and anatase are commercially important. In bulk form and with a large crystallite size, rutile is the thermodynamically stable form at normal pressure and at all temperatures up to its melting point. Anatase, which is typically the usual product in inorganic syntheses, can be transformed to rutile at elevated temperatures, the transformation being exothermic. With a very small crystallite size, anatase is shown to be the stable form, the critical size being around 11 nm in diameter, although smaller values have also been presented. Both rutile and anatase have a tetragonal unit cell and the structures can also be considered consisting of (TiO_6^{2-}) octahedra, which share edges and corners in rutile and edges in anatase as presented in Figure 1. Properties of the important TiO_2 polymorphs of rutile and anatase are presented in Table 1. (Kroschwitz & Howe-Grant 1997, Zhang & Banfield 2000b, Gopal et al. 1997)

Table 1. TiO_2 rutile and anatase structures and physical properties.

Property	Rutile	Anatase
Crystal structure	tetragonal	Tetragonal
Space group	$P4_2/mnm$	$I4_1/amd$
Lattice spacing a//c (nm)	0.459//0.296	0.378//0.951
Density (g/cm^3)	4.25	3.895
Refract. index, 550 nm	2.75	2.54
Band gap (eV)	3.05	3.25
Melting point (°C)	1830–1850	Conv. to rutile

The commercial properties of TiO_2 can be divided into pigmentary and non-pigmentary properties. The most important function of titanium dioxide is as a pigment for providing brightness, whiteness and opacity to such products as paints and coatings, plastics and rubber, paper products, cosmetics, tooth paste,

printing inks, fibers and food, as well as pottery and porcelain. This function is based on a high refractive index, a measure of the ability to bend light, of the rutile polymorph of titanium dioxide. From this is attained the opacity, the ability to hide. The growing number of pigment applications are in the field of UV-light pigments in sun-blocking for people and animals, protection of wood and plastics, food packaging, and coatings. Particle size is important for pigment applications; 200–300 nm particles exhibit a strong scattering of visible light wavelengths (400–600 nm) whereas 20–50 nm crystallites scatter ultraviolet spectrum of light (200–400 nm). The non-pigmentary applications utilize semiconducting and dielectric properties, high stability, and luminescence of TiO_2. Examples include a photovoltaic application in solar cells, a dominant position in photocatalyst applications for oxidizing pollutants (*e.g.* formaldehyde, cyanide, DDT, aromatics, surfactants, alkenes), gas sensors, electronic insulators, high temperature catalyst supports and ceramic membranes, and optoelectronic waveguides. (Jalava 2000, Blakey & Hall 1988, Honda & Fujishima 1972, O'Regan & Grätzel 1991, Frank & Bard 1977, Ollis et al. 1991, Ferroni et al. 1996, Campbell et al. 1999, Nair et al. 1997)

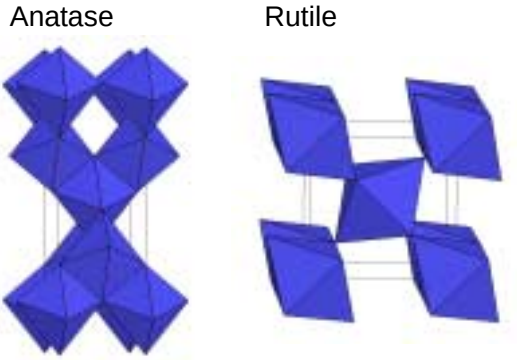

Figure 1. Anatase and rutile structures, pictured as consisting of (TiO_6^{2-}) octahedra.

Anatase is the usual product in inorganic syntheses. Anatase formation from an amorphous solid is reported to occur at around 400–450ºC (Oguri et al. 1988, Ohtani et al. 1997, Rodriguez-Talavera et al. 1997) and direct synthesis from a molecular precursor in solution is common knowledge (Gopal et al. 1997). The anatase to rutile transformation is a metastable to stable transition which has been studied for some decades (Czandera et al. 1958, Shannon & Pask 1965).

There is no unique transformation temperature but in the experimental studies the transition has occurred at 400–1000ºC with the rate and ignition temperature being critically dependent on synthesis conditions. The experimental phase diagram by Levin & McMurdie (1975), however, presents a transition temperature of 600ºC at normal pressure for bulk TiO_2. The list of conditions affecting the transformation is long. Defects (Kobata et al. 1991) as well as several kinds of impurities and dopants for which ionic radius and electric charge are notable properties (Iida and Ozaki 1961, MacKenzie 1975, Akhtar et al. 1992, Rodriguez-Talavera et al. 1997). Crystallite size is a factor affecting the transformation for which contradictory results have been presented, namely that decreasing crystallite size can increase anatase stability (Gribb & Banfield 1997) whereas commonly it is shown that anatase in such a finely crystallite size promotes transition to rutile (Suzuki & Tsukuda 1969, Ding et al. 1996, Ovenstone & Yanagisawa 1999, Xia et al. 1999, Kumar et al. 1993). Furthermore, conditions affecting the transformation are stoichiometry and reaction atmosphere (Shannon & Pask 1965, Iida & Ozaki 1961, MacKenzie 1975, Eastman 1994). Recently, particle attachment (Ahn et al. 1998), twin boundaries (Penn & Banfield 1999), and the presence of a secondary phase of brookite (Ovenstone and Yanagisawa 1999, Zhang & Banfield 2000b) have been reported to affect the anatase-to-rutile transformation rate, attributed to lattice strain due to adhesion. In addition, dislocations that can lead to complex polytypic and polymorphic structures are observed at the attachment of defect-free crystals (Penn & Banfield 1998).

It is well known that crystal morphology, *i.e.* crystal habit, minimizes the total surface free energy in the equilibrium shape of a crystal (Dirksen & Ring 1991). Natural mineral of anatase has {001} and {011} cleavage planes and shows steep pyramidal crystals, and rutile has {110}, {100} and {111} cleavage planes and shows prismatic short crystals (Roberts et al. 1990, Palache et al. 1944). Computational methods have been utilized to find the equilibrium morphologies of TiO_2 particles (Oliver et al. 1997). These simulations agree with electronic structure calculations (Ramamoorthy et al. 1994). The theoretical anatase morphology by atomistic simulation showed octahedra of {011} faces that are capped with {001} surfaces. Rutile showed {011}, {110}, {100}, and {221} faces. In addition, rutile is known to form needle-like structures in certain synthetic conditions (Li et al. 1999); a habit that is also observed in the nature.

2.2 Aerosol production of materials

Aerosol methods have been applied to the production of titanium dioxide particles in this thesis. An aerosol means a gas that contains particles that can be without any particular shape and crystallinity, or liquid droplets. Conventionally, the definition of an aerosol particle size is between 1 nanometer and 100 microns in atmospheric conditions (Friedlander 2000, Hinds 1999). An ultrafine particle size means a particle size range of <100 nm (Edelstein 1996, Ichinose et al. 1988). Powder means a group of particles after collection from the gas phase. The aerosol routes are advantageous in the preparation of particles with homogeneous composition as well as adjustable size, crystallinity, shape, and microstructure, to be utilized as bulk powder, single particles or deposited film (Messing et al. 1993, Gurav et al. 1993).

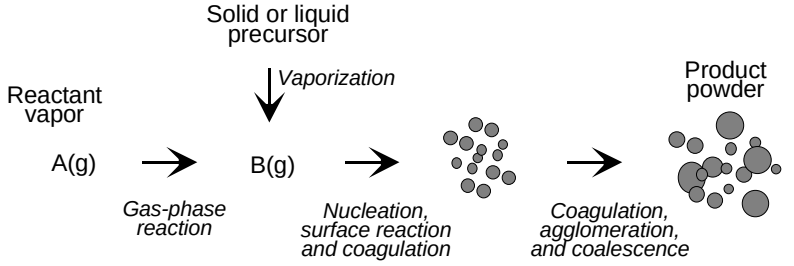

Figure 2. Schematic of gas-to-particle conversion process (adapted from Gurav et al. 1993).

The aerosol methods for producing particulate materials are generally divided into a gas-to-particle conversion and a liquid/solid-to-solid processing. In the gas-to-particle conversion, a supersaturated vapor of a gaseous species forms new particles. The vapor is formed either as a result of chemical reactions, *e.g*. thermolysis of a metal containing species that form metal oxide molecules with a very low saturated vapor pressure, or as a result of physical processes such as cooling that reduces the vapor pressure of condensable species. The supersaturation of gaseous species then leads to the formation of new particles by homogeneous nucleation (Figure 2). Usually processes such as particle collisions, vapor condensation on particles, coalescence, and agglomeration are caused by the high particle concentrations resulting from the gas-to-particle conversion. A relatively narrow particle size distribution, in terms of a geometric

standard deviation of around σ_g<1.5 is typically obtained. Several classes of materials have been formed by the gas-to-particle conversion. These include metals, oxide and non-oxide ceramics, and semiconductors. (Okuyama et al. 1986, Kodas 1989, Gurav et al. 1993, Kodas & Hampden-Smith 1999)

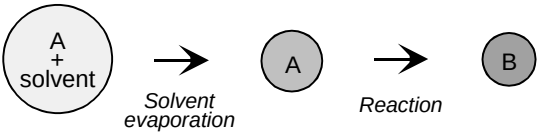

Figure 3. Schematics of droplet-to-particle synthesis of particles.

In the liquid/solid-to-particle processing, droplets or solid particles are converted to product particles via reaction either by thermolysis or with a carrier gas. In this thesis we refer to the method as aerosol decomposition when chemical reactions are involved. Other common names are spray pyrolysis, spray roasting, and spray calcination. In the case of no chemical reaction but merely drying, we call the conversion spray drying. The aerosol decomposition of a liquid precursor solution starts from the atomization of the solution and subsequent transportation of the formed droplets to the reactor. The reactor is often a hot-wall tube, as in this work, or a burner flame. In the aerosol decomposition synthesis solvent evaporates from the precursor solution droplets and product particles are formed by an intraparticle reaction within the particle as presented in Figure 3. Challenges to the method include volatile precursor and intermediate products that can evaporate and form additional particles by gas-to-particle conversion. This would lead to a bimodal size distribution. In the formation of product particles with such desired properties as morphology, porosity, crystallinity *etc*., controlling the reactor conditions is of high importance. The classes of materials produced by the method include inorganic materials such as metals, simple metal oxides, complex metal oxides, and non-oxides, as well as organic materials. (Sproson & Messing 1987, Kodas 1989, Messing et al. 1993, Gurav et al. 1993, Kodas & Hampden-Smith 1999)

2.3 Droplet-to-particle synthesis of TiO_2

The liquid/solid-to-particle synthesis of TiO_2 particles was studied in this project. In the literature, tubular flow reactors and flame reactors have been utilized of this task. Droplet dispersion has been generated by using spray nozzles, ultrasonic aerosol generators, nebulizers and electro-sprayers.

Pyrolysis synthesis of TiO_2, *i.e.* the decomposition of liquid droplets, has been reported to be achieved by using titanium alkoxides (Ishizawa et al. 1985, Park & Burlitch 1996, Murugavel et al. 1997, Bickmore et al. 1998), $TiCl_4$ aqueous solution (Lee et al. 1991), titanyl sulphate solution (Deguchi et al. 1994), and titanium citrate solution (Vallet-Regi et al. 1993). Crystalline titanium dioxide was not obtained in every case.

Hydrolysis of titanium tetrachloride droplets (Visca & Matijevic 1979) and alkoxide droplets (Visca & Matijevic 1979, Durand-Keklikian & Partch 1988, Rubio et al. 1997, Gablenz et al. 1998, Ingebrethsen & Matijevic 1984, Li et al. 1994, Kim et al. 2001) by water vapor has been reported as well as hydrolysis of alkoxide droplets with water included in the solution (Park & Burlitch 1992). Hydrolysis of alkoxides is a chemical process and can be performed at low temperatures but a post-calcination is typically required to achieve the titanium dioxide phase. As a low temperature process, the hydrolysis method can prevent excessive sintering and grain growth. Following on, the production of high specific surface area powders has been demonstrated. Hydrolysis of titanium alkoxides in sol-gel processes is commonly combined with various hydrolysis catalysts, for example, carboxylic acids (Doeuff et al. 1987).

The spray calcination of titanium species slurry has been performed (Gurav 1998, Ahonen et al. 2001). In this method, TiO_2 crystalline phase and crystallite size are controlled by reactor temperature and residence time where a colloidal solution of titanium species has been prepared earlier for dispersion.

3. Methods

Five different experimental systems were used to produce titanium dioxide powders and to study ultrafine particle formation and crystallization mechanisms. In all the experiments, precursor solution droplets were dispersed in a carrier gas of air or nitrogen, and transported to a tubular flow reactor where chemical (and physical) reactions formed solid titanium oxide particles. According to particle size, the experimental methods are divided into those with micron sized particles (Papers I–III) and those with ultrafine particles (Papers IV–V). The details of the systems are given in Papers I–V.

3.1 Powder production studies

In two studies of powder production (Papers I and II), the same reactor set-up was used while the precursor solution system was different. An ultrasonic aerosol generator (Langlet & Joubert 1992) was used for droplet dispersion. The dispersed droplet mass mean diameter was calculated according to Lang (1962). The air and nitrogen carrier gases had a flow rate of 10 lpm (20°C). The quartz reactor tube with 45 mm inner diameter (ID) had a heated length (l) of 65 cm. Droplets leaving the aerosol generator entered the heated volume of the reactor where solvent evaporated and, subsequently, chemical reactions formed solid particles. The particles were collected with an electrostatic precipitator. Subsequent to the collection, fractions of the powder samples were annealed at 500, 700 and 900°C for one hour in air. The aerosol mass size distributions were measured with a multi-stage low-pressure impactor (BLPI) (Hillamo & Kauppinen 1991). The as-prepared and annealed powders were characterized by X-ray diffraction (XRD), scanning electron microscopy (SEM), transmission electron microscopy (TEM), thermogravimetric analysis (TGA), Raman- and infrared (IR) spectroscopy, specific surface area (SSA) measurement, and X-ray fluorescence (XRF). The experimental set-up of Paper II is presented schematically in Figure 4.

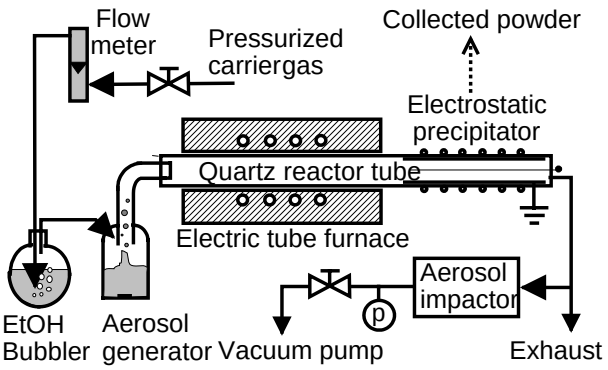

Figure 4. Experimental set-up for powder production by in-droplet hydrolysis (Paper II).

In the droplet pyrolysis experiments (Paper I), the powders were synthesized from a butanolic solution of titanium n-butoxide (TTNB). The calculated mass mean diameter of the droplets was 3.4 μm. Reactor wall temperatures between 200 and 580°C were used, which obtained average residence times from 4 to 2 seconds, respectively.

For the in-droplet hydrolysis experiments (Paper II), the precursor solutions were prepared from an ethanolic solution of titanium n-butoxide, acetic acid and water. The acetic acid replaced alkoxy ligands of the alkoxide (Barboux-Doeuff & Sanchez 1994) and the alkoxide was therefore chemically modified so as not to hydrolyze in bulk solution. An average droplet size of 3.3 μm was calculated. A reactor wall temperature of 200°C was used leading to an average residence time of 4 seconds.

The in-droplet hydrolysis at higher reactor temperatures and the TiO_2 crystallization *in-situ* in an aerosol reactor were studied (Paper III). The precursor solution was prepared similarly to that in Paper II. The reactor set-up consisted of an ultrasonic generator and a mullite reactor tube (ID=8 cm, *l*=91 cm). Nitrogen and air carrier gases had a flow rate of 5 l/min (20°C). The wall temperature was between 350 and 600°C resulting in average residence times between 26 and 18 seconds, respectively. The aerosol number size distributions were measured with a differential mobility analyzer (DMA) (Knutson & Whitby

1975, Wang & Flagan 1990) system, and the mass size distribution with BLPI. The powders and single particles collected were characterized by SEM, TEM, and XRD. Of the powder produced at 500°C in nitrogen, thin particle sections were prepared for microstructure investigation. This was obtained by casting a fraction of powder in epoxy and by thinning the sample mechanically and subsequently by ion milling. The specimen was transparent to electrons in TEM.

3.2 Investigation of ultrafine particles

In the studies of the ultrafine particle phase and structure formation (Papers IV and V), the experimental set-ups were similar according to droplet dispersion and size fractioning. The reactor modeling of the earlier pyrolysis experiment (Ahonen et al. 1998) had indicated that non-uniform temperature and flow profiles were obtained in the 45 mm diameter reactor. Therefore, better-controlled reactor conditions were attained by designing smaller, 22 mm diameter tube reactors; horizontally constructed in Paper IV and vertically in Paper V.

In the preparation of 60 and 120 nm TiO_2 particles (Paper IV), the precursor solution was made similarly to that of Paper II and III. The precursor solution was dispersed by an aerosol nebulizer and then dried to gain dry Ti-O particles. A fraction of the aerosol produced was mobility size classified with a DMA (Winklmeyer et al. 1991) into 100 and 200 nm diameter fractions. A monodisperse fraction was passed through a 22 mm diameter, horizontal tubular flow reactor with 0.3 l/min (20 °C) *air* flow rate. The heated reactor length of 60 cm at 20–1500°C supplied average residence times between 46 and 8 s. The particle size downstream of the reactor was measured with a second DMA, and lognormal distributions were numerically fitted to the measured number size distributions to present the particle size at each reactor temperature. Particle samples for TEM studies, including selected area (electron) diffraction (SAD) and microdiffraction, were collected.

The effects of flow development, heat transfer and buoyancy on particle trajectories were examined by performing computational fluid dynamics (CFD) calculations. Three-dimensional calculations of the reactor flow and temperature fields were performed by using the Fluent commercial CFD package (Fluent

Inc., Ver. 4.5). Computations took advantage of vertical symmetry perpendicular to the direction of gravity. Calculations were made at furnace wall temperatures of 500 and 1500°C.

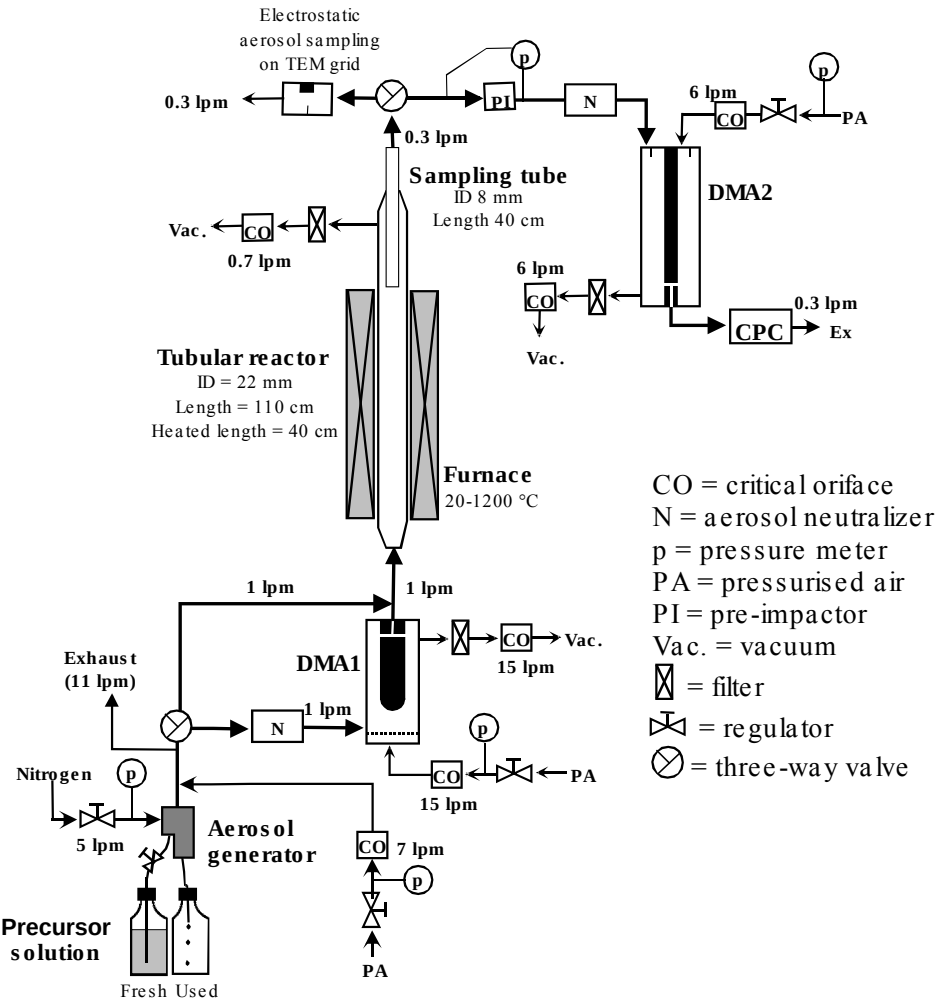

Figure 5. Experimental set-up of the investigation of 20 nm TiO_2 particles. (Paper V).

In studying 20 nm diameter TiO_2 particles (Paper V), titanium tetraisopropoxide (TTIP) in propanol was used as the precursor solution. The experimental set-up

is presented in Figure 5. An aerosol nebulizer was used. Following a dilution, the aerosol contained solid titanium dioxide hydrate particles after a hydrolysis reaction between TTIP and remnant water in propanol. The geometric mean diameter D_g of the particles was 40 nm with a geometric standard deviation σ_g of 1.8. The total number concentration n_{tot} was approximately $3 \cdot 10^6$ cm^{-3}. The aerosol was either directly transported to a tubular aerosol reactor or size classified to 40 nm diameter by a DMA. In the reactor, at *air* temperatures of 100–1200ºC, the particles were thermally decomposed and TiO_2 particles were formed. The residence time varied for 5 to 1 s at 200 to 1200ºC reactor temperature, respectively. A sample was taken from the reactor axis with a small tube, which provided an improved residence time control of sample particles compared to sampling from the whole reactor volume. The size distribution of the product particles was measured with a DMA. The morphology, microstructure, and crystal phase of the samples were studied with TEM.

The reactor conditions at the 800ºC reactor setting were calculated. The inner wall temperature of the reactor tube along the axial length was measured with real flow conditions and the temperature readings were used as the boundary conditions in the CFD calculations. Three-dimensional calculations of the reactor temperature and flow field were performed taking into account the buoyant forces. The calculations were made with the commercial computer code StreamWise (StreamWise Inc.).

4. Production and crystallization of micron-sized TiO_2 powders

The production of TiO_2 powders was accomplished by pyrolysis of alkoxide droplets (Paper I) and by in-droplet hydrolysis of alkoxide droplet solution (Paper II). The pyrolysis study was performed with an alcoholic solution of titanium alkoxide precursor in a flow tube reactor set-up. The same experimental set-up was also utilized with the in-droplet hydrolysis of alcoholic titanium alkoxide solution, including water. The in-droplet hydrolysis of titanium alkoxide droplets is a novel method for powder production whereas a hydrolyzing alkoxide solution is commonly utilized in sol-gel preparation of metal oxide powders and gels. The suitability of the in-droplet hydrolysis method to higher reactor temperatures and anatase crystallization *in-situ* in reactor conditions were investigated (Paper III). The experimental methods were presented in the chapter 3.1.

4.1 As-prepared powder properties

4.1.1 Morphology

The resulting powders' morphology was dependent on the reactor temperature and gas atmosphere. In pyrolysis of alkoxide droplets (Paper I), micron sized spherical particles were observed at 300ºC. The collected particles were separate when produced in air but they coalesced at collection when produced in nitrogen, indicating non-complete precursor decomposition. In pyrolysis at 500ºC in nitrogen, a large number of 30–80 nm particles were observed in addition to the micrometer-sized particles. This was due to evaporation of precursor species, subsequent oxidation to TiO_2 molecules, and ultrafine particle growth by collision and sintering. A bimodal size distribution was therefore observed. At 540 and 580ºC in air, some ultrafine particles were detected in addition to the micrometer-sized particles. SEM images of powder particles produced at 500ºC in air and nitrogen are presented in Figure 6.

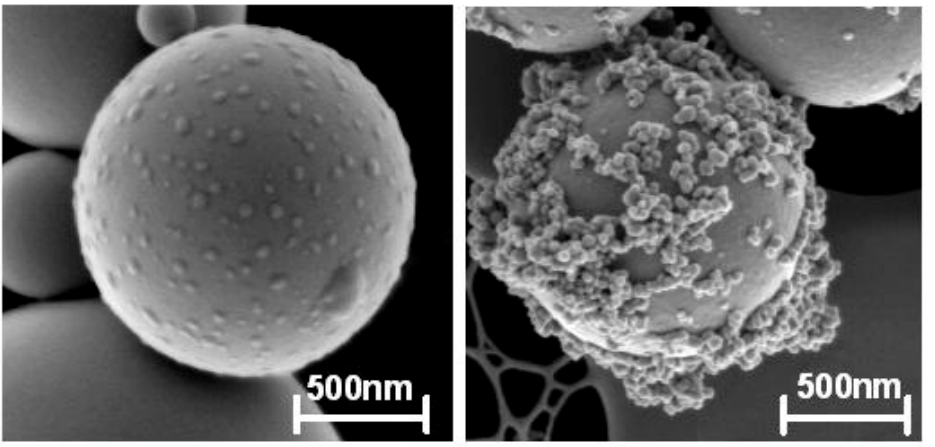

Figure 6. SEM images of powder particles produced by pyrolysis at 500ºC in air (left) and nitrogen (right)(Paper I).

The in-droplet hydrolyzed particles (Papers II and III) were smooth on the surface and either spherical or deflated; the degree of deflation was dependent on the precursor solution concentrations. A particle diameter larger than one micron increased the probability of deflated particles (Figure 7). The occurrence of the deflated, collapsed spheres was attributed to the polycondensation reaction of the precursor solution droplet initiated on the droplet surface. Evaporation of the ethanol solvent from the surface layer increased the relative concentrations of TTNB and water, and subsequently the polycondensation was accelerated. When the condensate layer had been formed, further drying, *i.e.* evaporation of the ethanol, from inside the particles led to a deflated particle shape.

Difference in particle morphology between air and nitrogen atmosphere was observed at high temperature as precursor species evaporated from the droplets at 500ºC in nitrogen. In addition, in air, solid particles were obtained at 300ºC whereas in nitrogen, partly liquid particles resulted. According to the TEM results there was no evidence of hollow particles either with spherical or deflated particles. Therefore the surface layer in all cases was flexible and permeable to allow vapor diffusion through the shell.

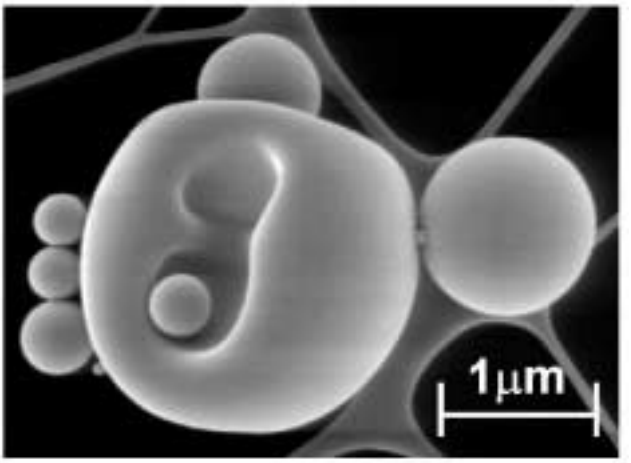

Figure 7. SEM image of powder particles produced by in-droplet hydrolysis at 200ºC (Paper II).

A specific surface area (SSA) as high as 279 m^2 g^{-1} was measured in the powder produced by pyrolysis in nitrogen, due to a large micropore area. Pyrolysis in air atmosphere, on the other hand, formed a much smaller SSA. The in-droplet hydrolysis in nitrogen formed a SSA of 144 m^2 g^{-1}, showing the adsorption isotherm of microporous material. In air, the in-droplet hydrolysis sample produced a SSA of 41 m^2 g^{-1} with the isotherm indicating non-porous or macroporous adsorbent. The different gas atmospheres therefore seem to supply a large difference in the SSA, attributed to the effect of oxygen. Oxygen is an active species during a hydrolysis process and thereby it increases polycondensation and reduces the SSA in air compared to an inert nitrogen atmosphere.

4.1.2 Particle size

The geometric mass mean diameter (aerodynamic) D_g / geometric standard deviation σ_g by BLPI was 2.3 μm/2.1 for pyrolysis in air, 2.1 μm/2.9 for pyrolysis in nitrogen, and 2.7 μm/1.8 for the in-droplet hydrolysis (Figure 8). The mass mode represented the particles formed from droplets. The largest size was observed with in-droplet hydrolysis, indicating the most vigorous reaction in the precursor droplet. Following on, the least vigorous reaction was indicated with pyrolysis in a nitrogen atmosphere. As the utilized titanium tetrabutoxide

precursor is volatile, the values of σ_g further indicate the different reactivities of the systems. The wider distribution is owing to the presence of ultrafine particles, also observed by SEM. Even though a volatile precursor was used at a high temperature it was obvious that the chemical reactions formed involatile species before any significant precursor evaporation. The results showed that using the same precursor solution concentration and aerosol generator, differing D_g's were observed. This can be explained by the fact that a more reactive atmosphere/condition produced larger particles that were less dense in structure. The eruption of some alkoxide species and the formation of ultrafine particles was later shown for in-droplet hydrolysis by DMA measurements (Paper III). The particles observed in the SEM images showed sizes in the micron range.

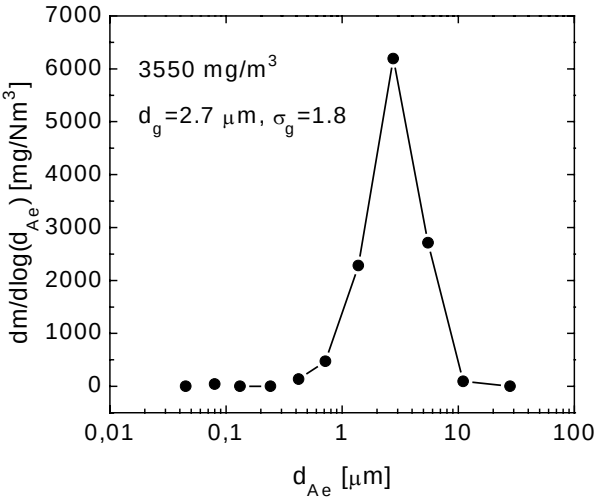

Figure 8. Mass size distribution of the in-droplet hydrolyzed particles in gas-phase (Paper II).

An example of the total mass concentration of 3550 mg/m^3 (Figure 8) presents the current set-up production scale of 2 g/h. It is commonly known that particle size and production rate in spray pyrolysis systems can be controlled by the choice of the dispersion method and solution concentration.

Investigation of the ultrafine particle formation at high temperatures with the in-droplet hydrolysis method was obtained by DMA measurements (Paper III). The number size distributions (NSD) in air showed unimodal distributions at 350 and

400°C with the mode at 250 nm as in Figure 9. The mode is attributed to particles formed from droplets. At 450°C the distribution had a lot of ultrafine particles. That is attributed to combustion of organic species in the particles and in the gas phase as well as a release of titanium species from the droplets to the gas phase together with bursting of particles, and a subsequent formation of ultrafine particles.

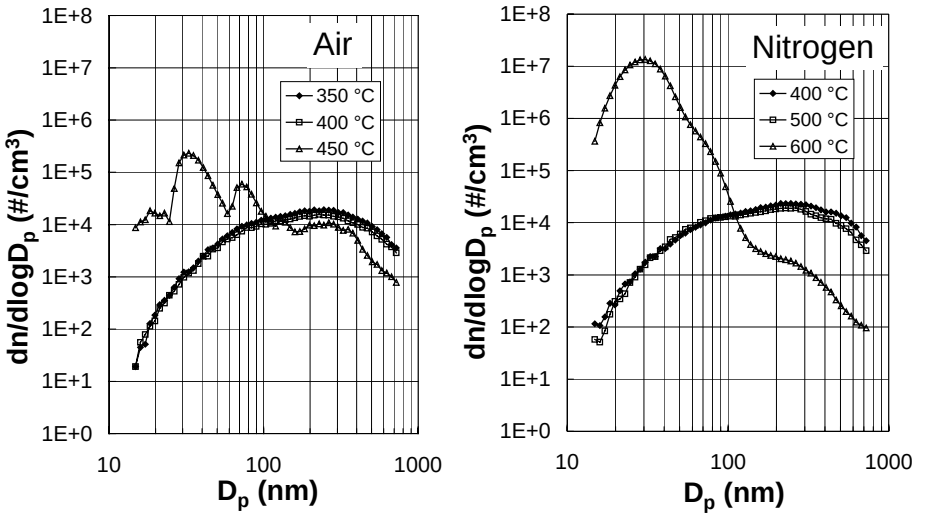

Figure 9. Number size distributions of the particles produced in air (left) and nitrogen (right) (Paper III).

The NSDs in nitrogen showed unimodal distributions at 400 and 500°C with the mode at 250 nm (Figure 9, right). At 600°C a large number of ultrafine particles was observed. This is attributed to evaporation (outgassing) of precursor species from inside the particles with a subsequent particle formation via gas-to-particle conversion.

4.1.3 Chemical composition

In the pyrolysis study (Paper I) the presence of butoxy groups was shown to decrease with increasing reactor temperature according to IR-spectroscopy. For the in-droplet hydrolysis samples (Paper II) the group vibrations in IR-spectra showed a large Ti-O band and O-H bands. No C-O bonds of alkoxide were

observed. Clearly observable metal-acetate chelating bonds were detected. The hydrolyzed powder samples corresponded to an intermediate state between TTNB and titanium oxo-hydrate formed via the hydrolysis reaction and the chelation with acetic acid. The butoxide groups were hydrolyzed with water, and the powders appeared to be Ti-O compounds with Ti-OH bonds and Ti-Ac chelating bonds.

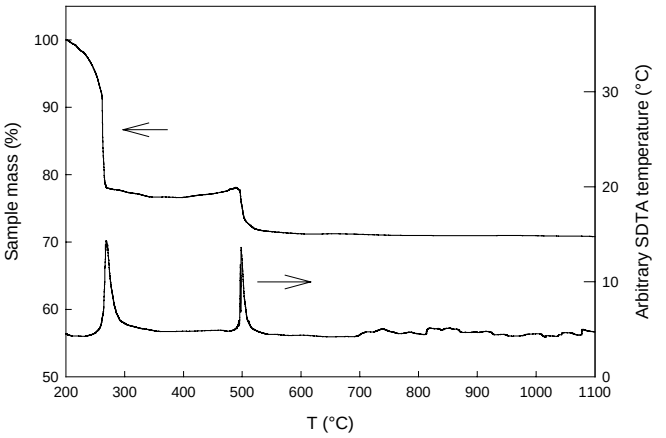

Figure 10. Thermogravimetric analysis of the powder produced by pyrolysis at 300ºC in nitrogen (Paper I).

The thermogravimetric analyses of the pyrolyzed and hydrolyzed samples at reactor temperatures of 200–300°C showed a major weight loss at 200–400°C, attributed to solvent evaporation and combustion (Papers I and II). The broad exothermic peaks on the SDTA curves coincided with the major weight loss and were attributed to the combustion of organic species. At 500°C the weight loss was attributed to dehydration of titanium oxyhydrate and the consequent formation of titanium dioxide, anatase (Figure 10). The powder pyrolyzed at 500°C in air showed mass loss in TGA only at 500°C and when pyrolyzed in nitrogen, no mass loss was seen in TGA.

4.1.4 Crystallinity

In the experiments, most of the collected powders were amorphous. Only in materials pyrolyzed at 500ºC in nitrogen and 580ºC in air (Paper I) as well as in in-droplet hydrolysis at 500ºC in nitrogen (Paper III) anatase peaks were observed by XRD. According to TEM, non-uniform crystallinity was observed in the powder produced by pyrolysis at 500ºC in nitrogen. The ultrafine particles were mostly amorphous (spot A in Figure 11) by ED image but nanocrystalline areas were found (spot B). The larger, spherical particles that were formed from droplets were similarly amorphous or crystalline. The inhomogeneity of the particle crystallinity indicated that reactor conditions, *i.e*. residence time and temperature, were not homogeneous for all particles. Based on CFD results (Ahonen et al. 1998), the flow fields and the temperature profiles within the reactor were complicated. The flow exhibited complex asymmetric behavior due to the combined effects of geometry and buoyancy which lead to large variations in the residence times and temperature histories experienced by individual particles. This is an obvious reason for the differences in particle properties, including the crystal structure development.

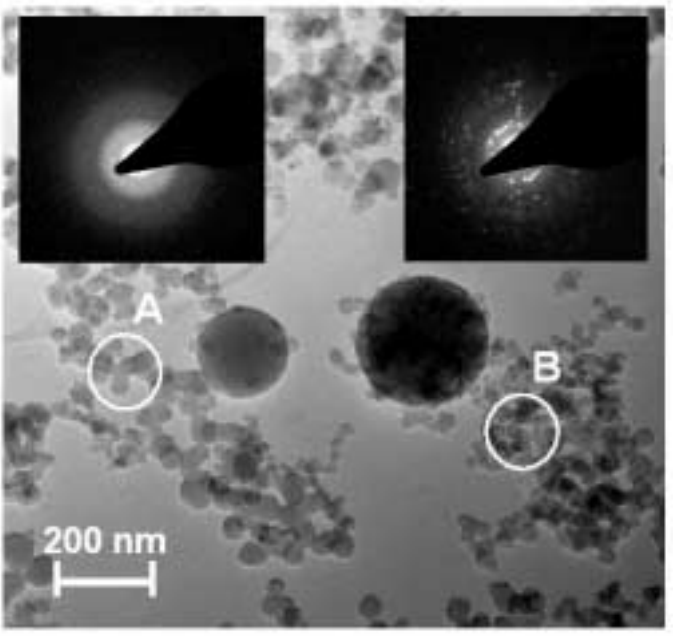

Figure 11. TEM image of powder produced at 500ºC in nitrogen (Ahonen et al., 1998).

Evidence of oxygen deficiency in the TiO_2 powder prepared at 500ºC in nitrogen was observed both by TEM and Raman spectroscopy (Paper I). It was possible to convert anatase particles to rutile in TEM with a high intensity electron beam. However, the sample did not convert to perfect rutile structure but instead a long-range periodic superstructure of rutile was observed. Long period superstructures, *i.e*. crystallographic shear planes, occur in reduced rutile crystals (Van Landuyt & Amelinckx 1970) and so oxygen deficient TiO_2 is indicated. The Raman spectroscopy signal exhibited a spectrum of anatase with the peak at 157.3 cm^{-1}. The shifted peak position from the 144 cm^{-1} of pure stoichiometric anatase indicated oxygen deficiency as shown by Parker and Siegel (1990). A stoichiometry of $TiO_{<1.88}$ was estimated.

During in-droplet hydrolysis at 500ºC in nitrogen (Paper III), an anatase structure was formed, according to XRD. A TEM image of the thinned sample is presented in Figure 12. The round particle images are thinned sections of powder particles, randomly cut off. Three Bright Field (BF) images of the same particle are presented with the sample tilted between the images. The tilting introduced

different diffracting conditions to the possible crystalline areas. The black areas within the particles represent crystallized parts where the crystal orientation is adapted to diffract electrons. The location of the diffracting areas differs from image to image indicating that the crystal orientations are not the same. Furthermore, the crystallized areas are separate and were therefore formed independently. The observed crystallized areas are located near the particle surface and are growing in a columnar way into the particles. Not all particles are identical in behavior, which is attributed to a heterogeneous thermal history of the particles in the reactor. The diffraction rings of a particle group (Figure 11, right, below) indicate the presence of polycrystalline anatase.

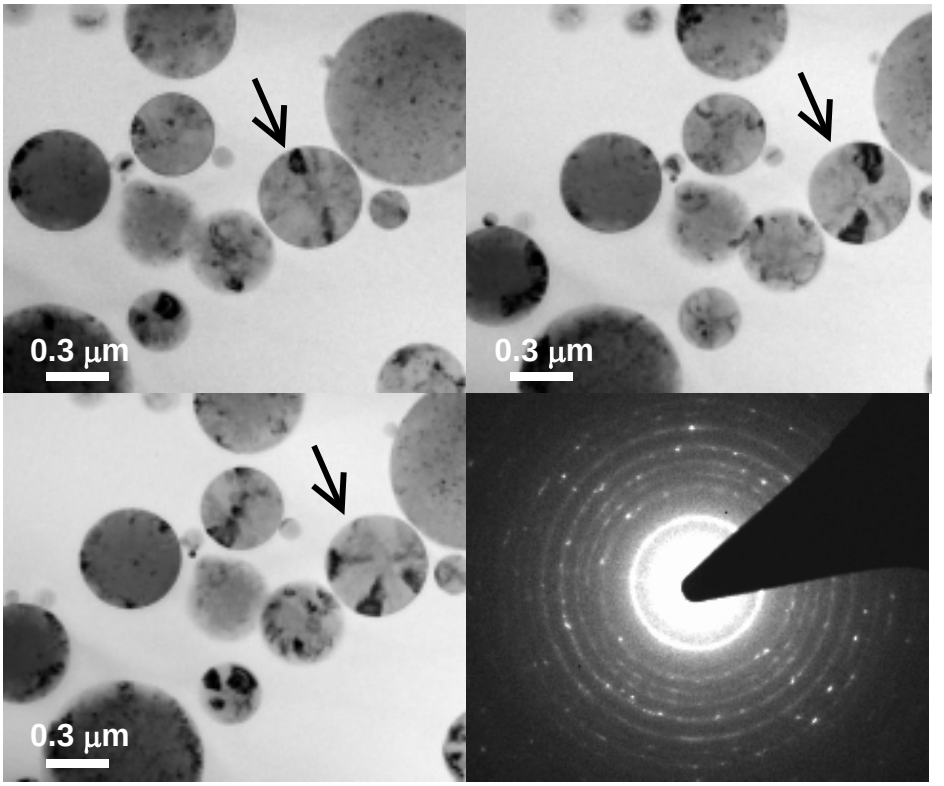

Figure 12. TEM images of particles with different diffraction conditions. Powder produced at 500ºC in nitrogen from an in-droplet hydrolysis precursor.

Particle surface is important in solid anatase nucleation. In the work of Yin et al. (1997) it was shown that the contact regions between neighboring particles

(touching each other in thermal annealing) are the likely nucleation sites for the anatase phase starting from amorphous particles. In the present study, the particles were separate in the gas phase and still multiple anatase nucleation events had occurred in the reactor. Surface energy is attributed as the reason for the observed crystal growth on surfaces as well as the fact that local impurities are known to promote conditions to initiate crystal nucleation.

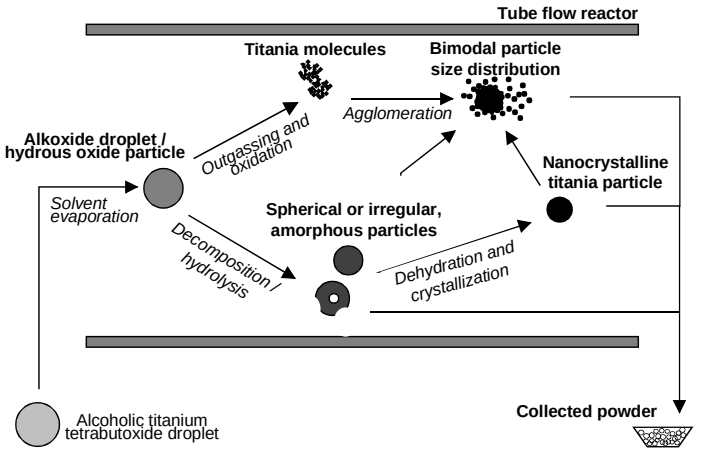

Figure 13. Physico-chemical phenomena during titanium dioxide powder production from metal alkoxide droplets in tube flow reactor.

The overall mechanism for titanium dioxide powder formation from metal alkoxide droplets is pictured in Figure 13. Solvent evaporates from the precursor solution droplet, which leads to the presence of either a metal alkoxide droplet or, in in-droplet hydrolysis, a hydrolyzed polycondensate particle. Possible evaporation of species can lead to formation of additional ultrafine particles via a gas-to-particle process and to a bimodal size distribution. Depending on the reactor temperature, the product powder can consist of TiO_2 or titanium dioxide hydrate. The appearance of residual species, *i.e.* organic ligands, decreases with increased temperature.

4.2 TiO_2 crystallization during thermal post-annealing

Collected powders produced by pyrolysis and in-droplet hydrolysis (Papers I and II) were subjected to thermal annealing. All powders annealed at 500°C were anatase (see for example Figure 14). The powders synthesized in a nitrogen atmosphere showed narrower peaks, indicating larger crystallites. When annealed at 700°C, both anatase and rutile phases were typically observed, except those powders produced by pyrolysis in nitrogen that were pure anatase. After annealing at 900°C, nearly phase-pure rutile was typically obtained. However, the powders produced by pyrolysis in nitrogen showed more stable anatase phases and, when pyrolyzed at 500°C, pure anatase was obtained even after one hour annealing at 900°C. The results indicate that there was a mechanism that retarded the anatase-to-rutile transformation in powders prepared in a nitrogen atmosphere. As presented in the previous chapter, oxygen deficiency of this powder was observed and this is considered to be the reason for the phase stability of anatase. On the other hand, an enhanced anatase-to-rutile transition was observed in one of the samples produced by in-droplet hydrolysis. Phase-pure rutile had already been formed during the annealing at 700°C, explained as an effect of solution preparation. A systematic investigation into the effect of the solution preparation conditions would be needed for further conclusions to be drawn.

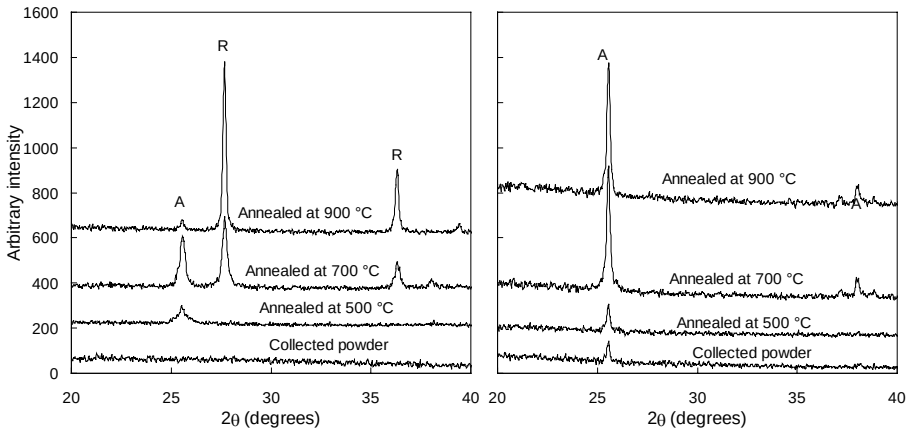

Figure 14. XRD patterns of collected powders, and after annealing. Powders synthesized by pyrolysis at 500ºC in air (left) and nitrogen (right) (Paper I).

The Raman spectroscopy signal of the sample pyrolyzed at 500°C in nitrogen and annealed for one hour at 900°C exhibited an anatase spectrum with the peak at 149.5 cm^{-1}. An estimated stoichiometry of $TiO_{1.97}$ shows that during the annealing, the TiO_2 anatase stoichiometry was approached, starting from $TiO_{<1.88}$ of the as-prepared powder, as presented previously.

5. Synthesis and crystallization of ultrafine TiO_2 particles

Mechanistic studies on the development of crystal morphology and phase transitions within ultrafine TiO_2 particles were carried out (Papers IV and V). Precursor solution droplets were nebulized and conveyed to a 22 mm diameter aerosol reactor where TiO_2 particles were produced at different temperatures *in air*. The experimental methods were presented in the chapter 3.2.

5.1 Particle production conditions

The CFD calculations of the 22 mm diameter *horizontal* flow reactor showed that the peak temperature *i.e*. the reactor wall temperature was reached by all particles entering the heated volume (Paper IV). The calculations were performed at temperatures of 500 and 1500°C for a 0.3 l/min air flow. The residence time distribution along the radial position is inevitable in a well-developed laminar flow. The flow exhibited complex vortix behavior near the reactor inlet and outlet due to the effect of buoyancy, but in the heated zone an approximately fully developed laminar flow was achieved. An average residence time calculation from the volumetric flow rate divided by the heated volume resulted in 17.3 and 7.6 seconds at 500 and 1500°C which is in good agreement with the CFD results.

The CFD results of the 22 mm diameter *vertical* reactor indicated that the velocity distribution was smooth, without large-scale recirculation or separation from the walls at 800°C (Paper V). Figure 15 shows the temperature distribution in the reactor tube. Also, the velocity distribution near the sampling tube is shown. There was a small low velocity recirculation zone at the centerline near the reactor inlet at low temperatures, below 260ºC. However, in the high temperature zone the flow became fully developed and the axial velocity approached a parabolic profile. Homogeneous temperature conditions were obtained. The calculated residence time of the sampled aerosol in the hot zone was between 0.98 and 0.71 s at the 800ºC reactor temperature.

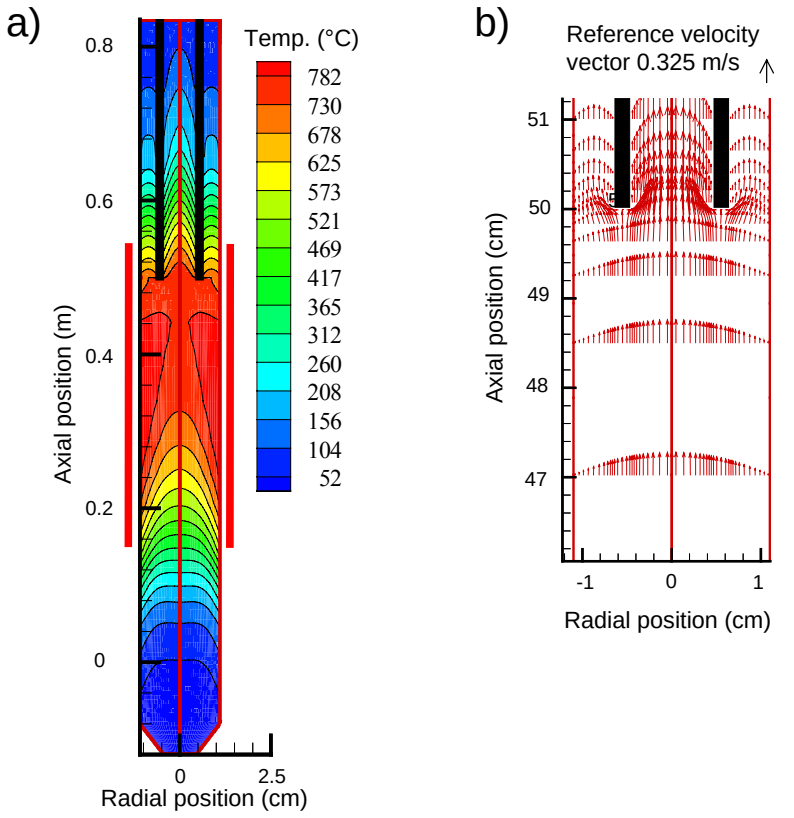

Figure 15. a) Temperature isotherms of the aerosol reactor at a 800ºC heated section wall temperature and air flow rate of 1 lpm (20ºC). b) Velocity vectors at the sample collection point. (Paper V)

5.2 Particle formation and mobility size development

The size development of the titanium dioxide particles at different reactor temperatures was investigated. Monodispersed 40, 100 and 200 nm diameter reactor inlet particles were pyrolyzed in the reactor in air carrier gas. The 40 nm particles were titanium isopropoxide derived and the 100/200 nm particles were titanium n-butoxide derived. The particle diameter decreased effectively as the reactor temperature went from room temperature up to 400ºC. Eventually, the minimum diameters of 20, 60 and 120 nm were observed at 600, 1000, and 1200ºC, respectively. At increased temperatures the mobility particle size increased slightly.

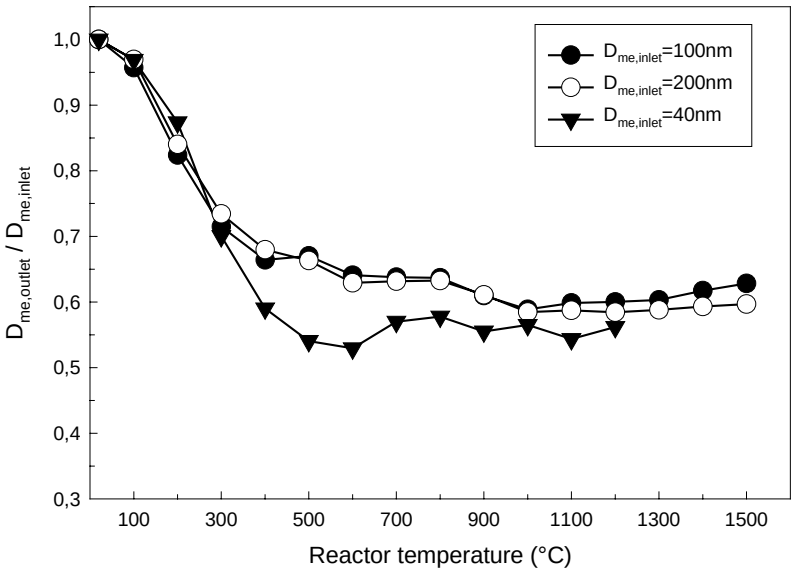

Figure 16. Ratio of reactor outlet and inlet mobility particle size at different reactor temperatures (100 and 200 nm data from Paper IV, and 40 nm data from Paper V).

Figure 16 graphically shows the relative size decrease of the particles as a function of the reactor temperature. The size decrease up to 400ºC was due to solvent release, *i.e*. drying, and due to combustion of organic species. Between 400 and 600ºC, an anatase phase was formed in the particles. According to TEM, the particles were single crystalline at the temperatures corresponding each measured minimum particle size, and at higher temperatures. In the 100 and 200 nm classified particles, the clear decrease in particle size between 800 and 1000ºC was due to densification and anatase-to-rutile phase transformation.

An increment in the mobility diameter of 60 and 120 nm diameter particles was observed above 1000 and 1200ºC, respectively, where single crystal particles were formed. For each crystal structure a crystal morphology, *i.e*. a characteristic shape of minimum energy at thermal equilibrium, exists. This is typically a non-spherical, faceted shape. On the other hand, the Stokes drag force, fundamental to DMA operation, is affected by a dynamic shape factor κ (Fuchs 1964). For nonspherical particles in a continuum regime the drag force depends on the shape and orientation, and is directly proportional to κ. For diffusable particles

the drag force further depends on the fluid slip. Kasper (1982) presented a set of basic relationships for the dynamic shape factor κ:

$$\kappa = \frac{D_{me}}{D_{ve}} \frac{C(D_{ve})}{C(D_{me})} = \kappa^{\circ} \frac{C(D_{ve})}{C(D_{me})} \quad (1)$$

where D_{me} is the mobility equivalent diameter, D_{ve} the volume equivalent diameter, $C(D_{me})$ and $C(D_{ve})$ the corresponding slip correction factors, and κ^{o} ($=D_{me}/D_{ve}$) the corresponding continuum regime dynamic shape factor.

By setting D_{ve} equal to the smallest measured mobility equivalent diameter, $D_{ve}=D_{me}$, κ equals unity which is the value for spherical particles. The assumption was validated by TEM. The dynamic shape factor for each temperature of increased mobility size was calculated. For 60 and 120 nm particles, the values of $\kappa^{o}=1.066$ and $\kappa^{o}=1.021$ ($\kappa=1.123$ and $\kappa=1.036$) were obtained at 1500ºC. The combined effect of particle elongation and facet formation is the reason for increased dynamic shape factor. In the Paper IV, corresponding dynamic shape factors by the prolate spheroid model (Davis 1979) were obtained at larger aspect ratios. This indicates the importance of the crystal corners to the dynamic shape factor.

5.3 Crystal morphology evolution

The TEM investigations showed that the spherical particles approached faceted shapes above the temperature where single crystalline particles were formed. Images of 60 nm diameter nanoparticles produced at reactor temperatures of 800, 1000, and 1300 ºC are shown in Figure 17 (Paper IV). At the reactor inlet, the size had been 100 nm. At 800 ºC, the 60 nm particles were composed of 15-20 nm crystallites. The overall shape of the particles was spherical but not smooth, owing to the visible shapes of the crystallites. The particles prepared at 1000 ºC were composed of a few crystallites with smooth surfaces. At 1300ºC, a clear faceted shape is observed on the particle that is a rutile single crystal. A similar trend was observed on the 120 nm diameter particles. An expected rutile crystal habit was shown by the fact that elongation was observed in the [001] direction.

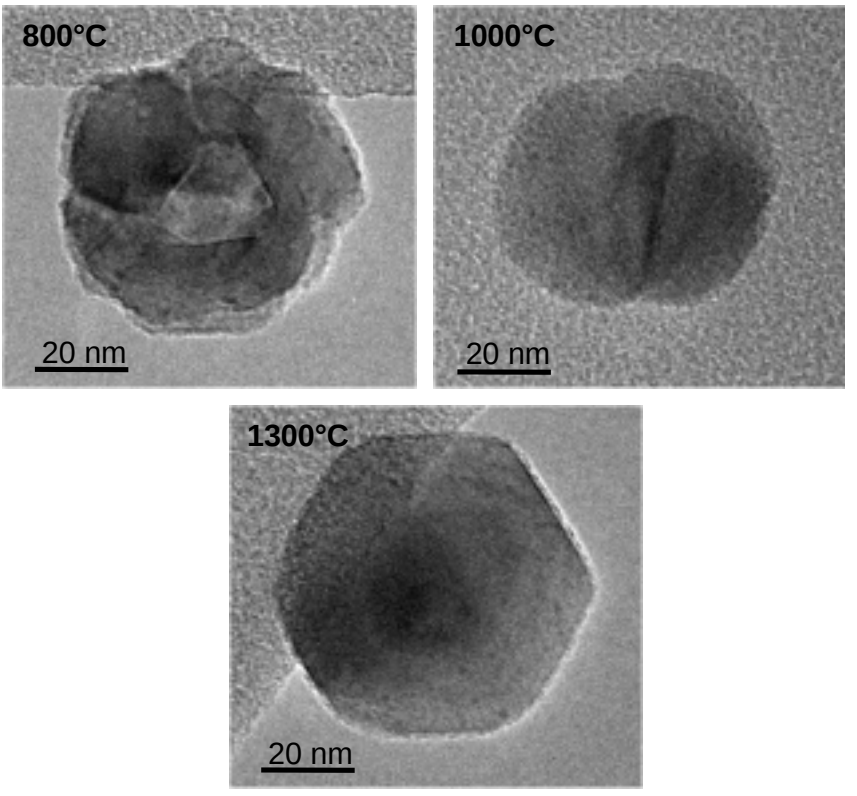

Figure 17. TEM images of 60 nm diameter particles produced at different reactor temperatures (Paper IV).

The shape of the 20 nm particles produced at 500 and 600ºC was spherical (Paper V). At 700 and 800ºC the shape was either irregular or spherical, whilst at 900ºC and above the particles were faceted. Polycrystalline morphology was not observed. At 600ºC and above the particles were single crystals. Examples of particles prepared at 600 and 1200ºC are presented in Figure 18.

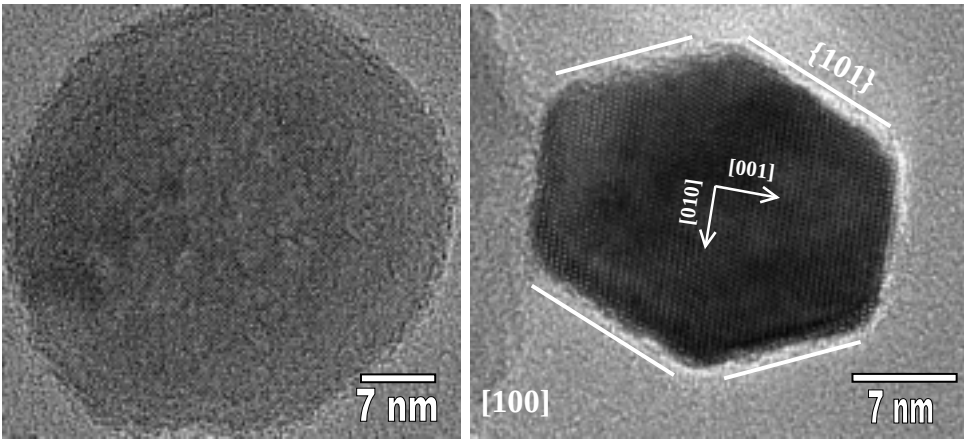

Figure 18. TEM images of polydisperse particles produced at 600ºC (left) and 1200ºC (right) (Paper V).

The shape of the well faceted anatase particles produced at 1200ºC, as exemplified in Figure 18, matches well with simulations by Oliver et al. (1997). Also, natural crystals show a similar shape (Palache et al. 1944). All the crystallographically indexed faceted particles indicated the presence of {101} and {001} faces. The particles were presumably approaching shapes of octahedra of {101} surfaces capped with {001} surfaces.

In order to investigate the importance of particle size for the appearance of faceted anatase particles, a set of additional experiments was carried out. By using the similar precursor solution to the Paper IV (Section 3.1) and otherwise the Paper V experimental (Section 3.2), we found out that the 20 nm particles at 1200ºC reactor temperature were faceted anatase particles, according to TEM. Therefore, because the result was the same as in Paper V, the particle size and not the precursor chemistry was important.

Figure 19 summarizes schematically our findings concerning the precursor droplet transformation to a faceted TiO_2 particle, and the main intermediate stages. In formation of faceted anatase particles the presence of single crystalline anatase particles at lower temperatures was observed (Paper V). When phase change to rutile was initiated at polycrystalline stage then transformation to rutile was observed at 800–1000ºC (Paper IV). The crystal-crystal attachment promotes anatase-to-rutile transformation and therefore it is important to attain

single crystalline anatase at fairly low temperatures (<700–800ºC), if faceted anatase is targeted. Within this study 20 nm titanium dioxide particles turned out to form single crystalline anatase whereas in 60 nm and larger particles the phase transition to rutile started at polycrystalline stage. Small particle size is advantageous in forming single crystalline anatase by sintering but, in principle, a longer residence time would form single crystalline anatase similarly of larger particles. The faceted anatase crystallites showed increased thermal stability up to 1200ºC regarding the anatase-to-rutile transformation.

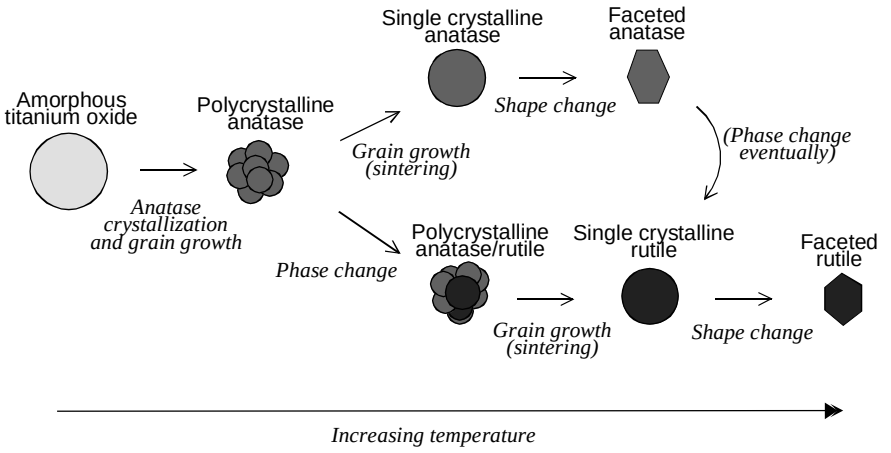

Figure 19. Mechanisms of ultrafine titanium dioxide particle crystallization.

The single crystalline TiO_2 particles in the aerosol reactor can be useful model particles for studying the transformation of anatase to rutile via solid phase nucleation. For example, in a recent article three models for solid rutile nucleation were proposed: interface nucleation, surface nucleation, and bulk nucleation (Zhang and Banfield 2000a). By using single crystalline particles in the gas phase, the interface nucleation could be neglected in an experiment and further modeling.

5.4 Titanium dioxide phase development

The 20 nm diameter particles were anatase (Paper V). According to selected area diffraction (SAD) ring patterns of particle groups, and Fourier transform images of numerous HR-TEM images, anatase was present in reactor temperatures from

500ºC up to 1200ºC. Only a few diffraction spots by SAD indicated the presence of rutile crystallites at 1200ºC (Figure 20). In addition, one HR-TEM image was indexed with a rutile structure. Also, larger than 20 nm diameter particles investigated (<40 nm) were anatase.

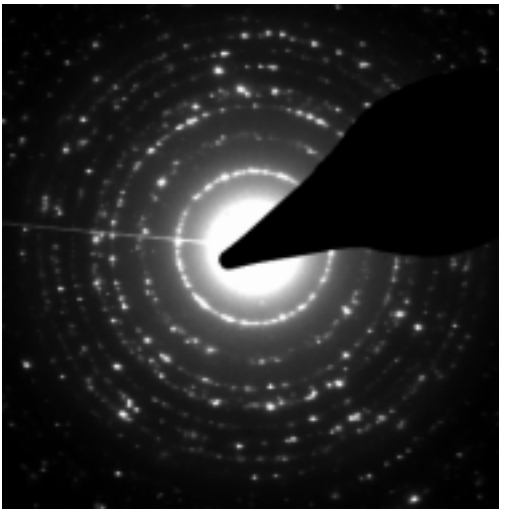

Figure 20. Selected area diffraction ring pattern of anatase particles (Paper V).

In the 60 and 120 nm diameter polycrystalline particles, anatase was observed appearing at a 600ºC reactor temperature, and a gradual transformation to rutile occurred between 800 and 1000ºC. The electron microdiffraction patterns obtained from the 800ºC sample of selected crystallites showed that anatase and rutile crystals were present within the given particles in approximately the same amounts (Figure 21). Most of the crystallites in the particles prepared at 1000 ºC were rutile, according to the electron microdiffraction patterns (Figure 22). Only a few electron diffraction patterns of the separate crystallites were indexed with the anatase crystallographic structure. At higher reactor temperatures only the rutile phase was present.

The 20 nm diameter particles can be considered to be of a thermally stable anatase structure. With only a slight indication of rutile formation even at 1200ºC, there was a reason for the thermal stability of anatase, *i.e*. retarding rutile nucleation. The reason for anatase stability is attributed to appearance of single crystal particles already at a relatively low temperature of 600ºC,

chemical purity, and absence of crystal-crystal attachment. Impurities are a well-known and important promotor of anatase-to-rutile transformation. The faceted morphology leads to a minimized surface energy and an increased activation energy of the A→R transformation, which may be of importance at temperatures >1000ºC. Particle size is commonly known as a factor affecting A→R transition but with a decreased particle size, as in this study, rather a lowered A→R transformation temperature is expected. In addition, smaller than 20 nm particles have been observed to transform to rutile. In this study, neither particle-particle nor crystal-crystal attachment that are known promotors of the transition (Zhang & Banfield 2000a) was present.

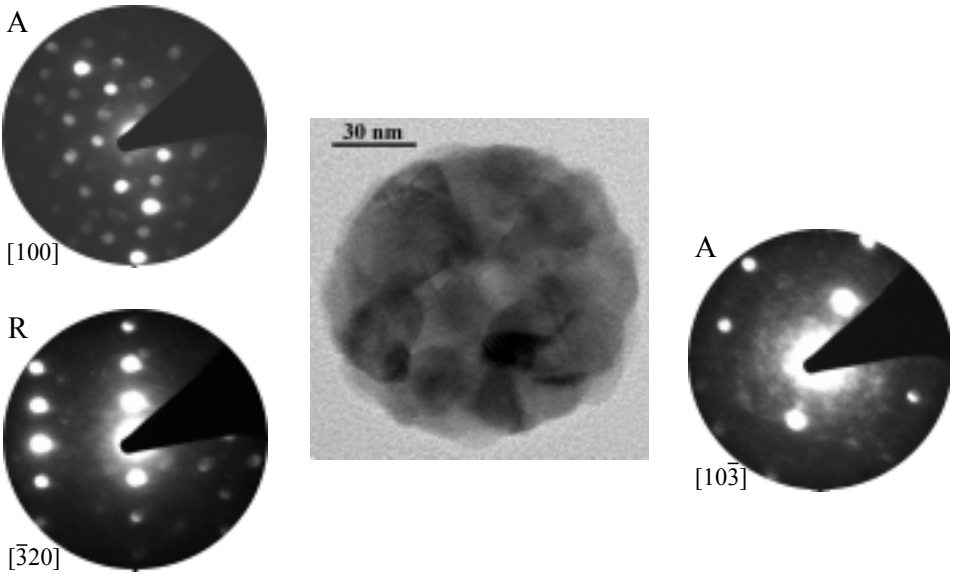

Figure 21. Microdiffraction patterns of selected crystallites within a TiO_2 particle prepared at 800 ºC (courtesy by Olivier Richard).

The 60 and 120 nm diameter particles transformed into rutile at the temperature range of 800–1000ºC. Commonly, the transition occurs between 600 and 1000ºC and above 730ºC the transition rate is considered rapid (Czandera et al. 1958). In aerosol reactor studies with alkoxide precursor and similar grain sizes, the phase change from anatase to rutile has been observed beginning at temperatures between 700–850ºC. It is concluded that the rutile phase within 60 and 120 nm diameter particles was formed as expected at 800ºC. When compared with the

20 nm diameter particles, it is to be noted that precursor solution preparation is commonly known to effect on crystal formation.

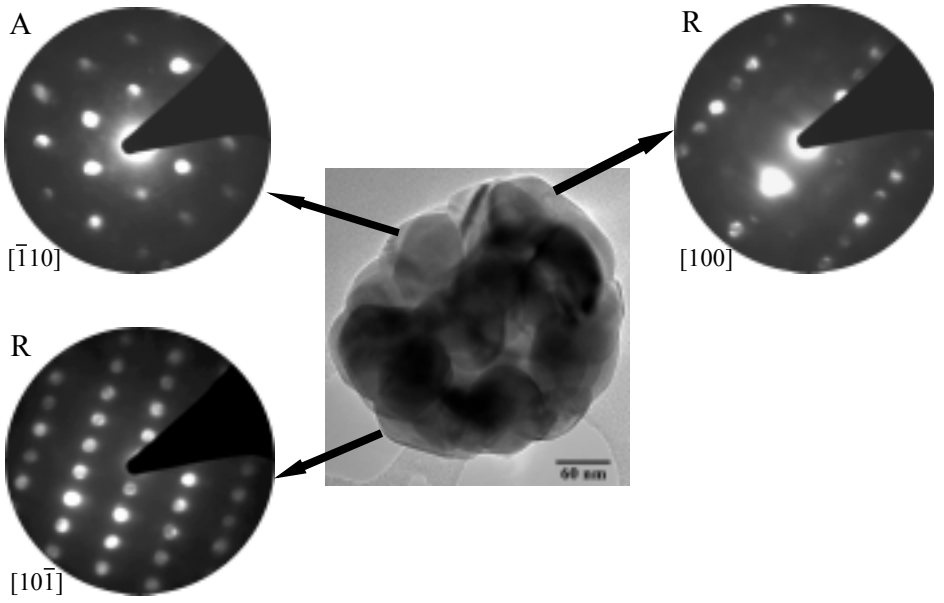

Figure 22. Microdiffraction patterns of selected crystallites within a TiO_2 particle prepared at 1000ºC (courtesy by Olivier Richard).

6. Summary

The aerosol production of titanium dioxide particles has been studied in this thesis in order to develop particle production methods and to gain understanding of crystallization mechanisms. Titanium alkoxide precursors in alcoholic solutions were used in a droplet-to-particle synthesis route. Tubular flow reactors were used in the experiments. Computational modeling of the reactor flow and temperature profiles was performed for developing well-controlled reactor conditions. Both micron-sized and ultrafine titanium dioxide particles were produced and characterized by aerosol measurements, electron microscopy, and materials characterization. Different reactor temperatures were used to create a mechanistic picture of the physico-chemical processes involved and to contribute to the development of titanium dioxide production methods.

A pyrolytic route for titanium dioxide powder production was used and further developed. The decomposition of titanium tetrabutoxide droplets produced gram quantities of micron-sized powder. The powder production at 300°C in air and nitrogen atmospheres formed amorphous titanium oxide. At 500°C in nitrogen, an anatase phase was formed *in-situ* and this powder turned out to be anatase even after one hour thermal annealing in air at 900°C. The sample was further observed to be oxygen-deficient titanium dioxide, which is given as the reason for the presence of phase-stable anatase. Formation of additional ultrafine particles via gas-to-particle synthesis from evaporated species was observed above 400°C. Nanocrystalline titanium dioxide powders were formed in subsequent thermal annealings.

A novel precursor system for titanium dioxide powder production was introduced by using a sol-gel type solution, including water, and dispersing it for droplet hydrolysis. Each droplet formed a micro-reactor for hydrolysis with particle synthesis conditions being determined by the flow reactor used. Gram quantity production of micron-sized titanium oxo-hydrate powders was demonstrated. The particles produced at 300°C contained remnants of the hydrolysis catalyst, acetic acid. Nanocrystalline titanium dioxide powders of anatase and rutile were formed in subsequent thermal annealings. When produced at 450°C in air and at 600°C in nitrogen, additional ultrafine particles via gas-to-particle synthesis from outgassed species were formed. In addition to the powder production, single 60 and 120 nm diameter titanium dioxide particles

were prepared with in-droplet hydrolysis and simultaneously crystallized in an aerosol reactor up to 1500°C in air. Anatase crystallization on amorphous particles in the reactor was shown to occur near the particle surfaces. Separate crystallites were observed in submicron sized particles that were prepared at 500°C in nitrogen via the in-droplet hydrolysis method.

Mechanistic studies on crystallization of ultrafine titanium dioxide particles were performed using a 22 mm diameter tubular, laminar flow aerosol reactor. The computational fluid dynamics results showed that both the horizontal and vertical set-up produced a uniform flow and temperature profile in the heated zone. These conditions were considered adequate for a droplet-to-particle synthesis method.

Titanium dioxide particles of 60 and 120 nm diameter became single crystalline rutile at 1000 and 1200ºC reactor temperatures, respectively. At higher temperatures, the mobility equivalent diameters of the constant volume particles increased. This was due to the crystal habit formation that created faceted, elongated particles and subsequently an increased dynamic shape factor. At a reactor temperature of 1500ºC, a continuum regime dynamic shape factor of 1.07 for 60 nm particles and 1.02 for 120 nm particles was determined. The calculation of the dynamic shape factor can therefore be used in monitoring the development of crystal morphology of single crystalline particles. The titanium dioxide particles consisted of nanocrystalline anatase at 600ºC, a mixture of 20 nm anatase and rutile crystallites at 800ºC, 50–60 nm crystallites of almost phase pure rutile at 1100ºC, and single crystal rutile particles with a clear crystal habit at 1300 and 1500ºC.

In a separate study, 20–40 nm diameter titanium dioxide particles were studied. Partly amorphous and partly crystalline anatase particles were observed at a 500ºC reactor temperature and single crystalline anatase at 600–1200ºC. The stability of the anatase phase even at 1200ºC is attributed to defect-free particles, lack of crystal-crystal attachment, and faceted shape that promoted a lower total energy. Subsequently, the conditions were provided that inhibited the anatase-to-rutile transition that normally is expected between 700–900ºC in alkoxy derived particles. The anatase crystal morphology had {101} and {001} surfaces. The separated nanoparticles via droplet-to-particle synthesis routes are good model

particles for studying titanium dioxide crystallization *e.g.* crystal morphology development and the anatase-to-rutile nucleation process.

Further studies to continue this work are proposed. The *precursor* and the solution conditions offer several aspects to study as they affect on the crystal structure of the resulting powder. In this study, the anatase to rutile transformation temperature indicated to be strongly dependent on the precursor solution preparation. The *process* of the in-droplet hydrolysis and its modeling would be another interesting piece of work, including how a hollow morphology can be avoided in the resulting powders. Yet another study is to look for the actual position of rutile nucleation on single crystalline anatase particles. And to gain kinematic data on the anatase-to-rutile transformation of the aerosol particles at different temperatures would be of great interest for modeling in future. The *product* related aspects like the desired properties also offer possible studies. Control on the particle morphology is interesting and, *e.g.*, preparation of >10 μm diameter particles where alkoxide droplet hydrolysis by using water vapor would be stopped by the forming TiO_2 shell (Li et al. 1994). A large increase in the produced mass would be gained compared with micron-sized droplets.

References

Ahn, J.-P., Park, J.-K., Kim, G. 1998. Effect of compact density on phase transition kinetics from anatase phase to rutile phase during sintering of ultrafine titania powder compacts. NanoStructured Materials, Vol. 10, pp. 1087–1096.

Ahonen, P., Brown, D., Kauppinen, E., Tapper, U., Jokiniemi, J., Deschanvres, J.L., Joubert, J.C., Van Tendeloo, G. 1998. Preparation of Titania via Aerosol Decomposition in Tube Flow Reactor: The Effect of Reactor Flow Conditions. In: M. C. Roco, S. Pratsinis and S. Beaucage (eds.). Advanced Technologies for Particle Processing. Vol. 1. Proceedings of the AIChE Annual Meeting, Particle Technology Forum, Symposium A, Miami Beach, FL, USA, Nov 15–20, 1998. Pp. 205–210.

Ahonen, P. P., Moisala, A., Richard, O., Kauppinen, E. I., Brown, D. P., Jokiniemi, J. K., Jalava, J.-P. Kurki, K. 2001. Spray calcination of titanium dioxide. PARTEC 2001 Congress Proceedings, Nuremberg, Germany, March 27–29.

Akhtar, M.K., Pratsinis, S. E., Mastrangelo, S. V. R. 1992. Dopants in vapor-phase synthesis of titania powders. J. Am. Ceram. Soc., Vol. 75, pp. 3408–3416.

Barboux-Doeuff, S., Sanche, C. 1994. Synthesis and characterization of titanium oxide-based gels from acetate modified titanium butoxide precursors. Mat. Res. Bull., Vol. 29, pp. 1–13.

Bickmore, C. R., Waldner, K. F., Baranwal, R., Hinklin, T., Treadwell, D. R., Laine, R. M. 1998. Ultrafine titania by flame spray pyrolysis of a titanitrate complex. J. Eur. Ceram. Soc., Vol. 18, pp. 287–297.

Blakey, R. R., Hall, J. E. 1988. Titanium dioxide. In: Lewis, P. A. (ed.). Pigment handbook. Vol. 1. John Wiley & Sons, Inc., New York.

Campbell, S. A., Kim, H.-S., Gilmer, D. C., He, B., Ma, T., Gladfelter, W. L. 1999. Titanium dioxide (TiO_2)-based gate insulators. IBM J. Res. Develop., Vol. 43, pp. 383–392.

Czanderna, A.W., Rao, C. N. R., Honig, J. M. 1958. The anatase-rutile transition. Trans. Farad. Soc., Vol. 54, pp. 1069–1073.

Davis, C. N. 1979. Particle-fluid interaction. J. Aerosol Sci., Vol. 10, pp. 477–513.

Deguchi, S., Matsuda, H., Hasatani, M., Kobayashi, N. 1994. Formation mechanism of TiO_2 fine particles prepared by the spray pyrolysis method. Drying Technology, Vol. 12, pp. 577–591.

Ding, X.-Z., Liu, X.-H., He, Y.-Z. 1996. Grain size dependence of anatase-to-rutile structural transformation in gel-derived nanocrystalline powders. J. Mater. Sci. Lett., Vol. 15, pp. 1789–1791.

Dirksen, J. A., Ring, T. A. 1991. Fundamentals of crystallization: kinetic effects on particle size distributions and morphology. Chem. Eng. Sci., Vol. 46, pp. 2389–2427.

Doeuff, S., Henry, M., Sanchez, C., Livage, J. 1987. Hydrolysis of titanium alkoxides: modification of the molecular precursor by acetic acid. J. Non-Cryst. Sol., Vol. 89, pp. 206–216.

Durand-Keklikian, L., Partch, R. E. 1988. Microencapsulation of oil droplets by aerosol techniques. – 1. Metal oxide coatings. J. Aerosol Sci., Vol. 19, pp. 511–521.

Eastman, J. A. 1994. Microstructural development in nanophase TiO_2 during annealing. J. Appl. Phys., Vol. 75, pp. 770–779.

Edelstein, A. S. (ed.) 1996. Nanomaterials: synthesis, properties and applications. Institute of Physics Publishing, Bristol. 596 p.

Ferroni, M., Guidi, V., Martinelli, G., Faglia, G., Nelli, P., Sberveglieri, G. 1996. Characterization of a nanosized TiO_2 gas sensor. NanoStructured Materials, Vol. 7, pp. 709–718.

Frank, S. N., Bard, A. J. 1977. Heterogeneous photocatalytic oxidation of cyanide and sulfite in aqueous solutions at semiconductor powders. J. Phys. Chem., Vol. 81. pp. 1484–1488.

Friedlander, S. K. 2000. Smoke, dust and haze. 2nd ed. Oxford University Press, New York.

Fuchs, N.A. 1964. The Mechanics of Aerosols. Pergamon Press Ltd.

Gablenz, S., Völtzke, D., Abicht, H.-P., Neumann-Zdralek, J. 1998. Preparation of fine TiO_2 powders via spray hydrolysis of titanium tetraisopropoxide. J. Mater. Sci. Lett., Vol. 17, pp. 537–539.

Gopal, M., Moberly Chan, W. J., De Jonghe, L. C. 1997. Room temperature synthesis of crystalline metal oxides. J. Mater. Sci., Vol. 32, pp. 6001–6008.

Gribb, A. A., Banfield, J. F. 1997. Particle size effects on transformation kinetics and phase stability in nanocrystalline TiO_2. Amer. Mineralogist, Vol. 82, pp. 717–728.

Gurav, A. 1998. Aerosol processing of materials: Aerosol dynamics and microstructure evolution. PhD dissertation, University of New Mexico. 152 p.

Gurav, A., T. Kodas, T. Pluym, Y. Xiong. 1993. Aerosol processing of materials. Aerosol Sci. Tech., Vol. 19, pp. 411–452.

Hillamo, R. E., Kauppinen, E. I. 1991. On the performance of the Berner low-pressure impactor. Aerosol Sci. Tech., Vol. 14, pp. 33–47.

Hinds, W. C. 1999. Aerosol technology: properties, behavior and measurement of airborne particles. 2nd edition. John Wiley & Sons, New York. 483 p.

Honda, K., Fujishima, A. 1972. Electrochemical photolysis of water at a semiconductor electrode. Nature, Vol. 238, pp. 37–38.

Ichinose, N., Ozaki, Y., Kashu, S. 1988. Superfine particle technology. Springer-Verlag, London.

Iida, Y., Ozaki, S. 1961. Grain growth and phase transformation of titanium oxide during calcination. J. Am. Ceram. Soc., Vol. 44, pp. 120–127.

Ingebrethsen, B. J., Matijević, E. 1984. Kinetics of hydrolysis of metal alkoxide aerosol droplets in the presence of water vapor. J. Coll. Interf. Sci., Vol. 100, pp. 1–16.

Ishizawa, H., Sakurai, O., Mizutani, N., Kato, M. 1985. Preparation and formation mechanisms of TiO_2 fine particles by spray pyrolysis of metal alkoxide. Yogyo-Kyokai-Shi, Vol. 93, pp. 382–386.

Jalava, J.-P. 2000. Formation of TiO_2 pigment particles in the sulphate process – a methodological study. PhD dissertation, University of Turku.

Joutsensaari, J. 1999. Aerosol synthesis of nanostructured, ultrafine fullerene particles. PhD dissertation, Tampere University of Technology.

Kasper, G. 1982. Dynamics and measurement of smokes. I, Size characterization of nonspherical particles. Aerosol Sci. Tech., Vol. 1, pp. 187–199.

Kim, J., Wilhelm, O., Pratsinis, S. E. 2001. Nanostructured porous titania powders by sol-gel peptization and spray drying. PARTEC 2001 Congress Proceedings, Nuremberg, Germany, March 27–29.

Knutson, E. O., Whitby, K. T. 1975. Aerosol classification by electrical mobility: apparatus, theory and applications. J. Aerosol Sci., Vol. 6, pp. 443–451.

Kobata, A., Kusakabe, K., Morooka, S. 1991. Growth and transformation of TiO_2 crystallites in aerosol reactor. AIChE J., Vol. 37, pp. 347–359.

Kodas, T. T. 1989. Generation of complex metal oxides by aerosol processes: superconducting ceramic particles and films. Angewandte Chemie International Edition, Vol. 28, pp. 794–807.

Kodas, T. T., Hampden-Smith, M. 1999. Aerosol processing of materials. Wiley-VCH, New York.

Kroschwitz, J. I., Howe-Grant, M. 1997. Kirk Othmer encyclopedia of chemical technology. 4th ed. Vol. 24. John Wiley & Sons, New York.

Kumar, K.-N. P., Keizer, K., Burggraaf, A. J. 1993. Textural evolution and phase transformation in titania membranes: Part 1. – Unsupported membranes. J. Mater. Chem., Vol. 3, pp. 1141–1149.

Lang, R. J. 1962. Ultrasonic atomization of liquids. J. Acoust. Soc. Am., Vol 34. pp. 6–8.

Langlet, M., Joubert, J.C. 1992. The pyrosol process or the pyrolysis of an ultrasonically generated aerosol. In: C. N. R. Rao. Chemistry of Advanced Materials. Blackwell Scientific Publications, Oxford. Pp. 55–76.

Lee, J.-H., Cho, H.-J., Park, S.-J. 1991. Preparation of spherical TiO_2 particles by ultrasonic spray pyrolysis. In: Messing, G. L., Hirano, S., Hausner, H. (eds.). Ceramic transactions. Vol. 22: Ceramic powder science. American Ceramic Society, Westerville. Pp. 39–44.

Levin, E. M., McMurdie, H. F. 1975. Phase diagrams for ceramists: 1975 supplement. American Ceramic Society, Columbus (Ohio).

Li, W., Rassat, S. D., Foss, W. R., Davis, E. J. 1994. Formation and properties of aerocolloidal TiO_2-coated microspheres produced by alkoxide droplet reaction. J. Coll. Interf. Sci., Vol. 162, pp. 267–278.

Li, G.-L., Wang, G.-H., Hong, J.-M. 1999. Morphologies of rutile form TiO2 twins crystals. J. Mater. Sci. Lett., Vol. 18, p. 1243–1246.

MacKenzie, K.J.D. 1975. The effect of reaction atmosphere and electric fields on the anatase-rutile transformation. Trans. J. Br. Ceram. Soc., Vol. 74, pp. 121–125.

Messing, G. L., Zhang, S.-C., Jayanthi, G. V. 1993. Ceramic powder synthesis by spray pyrolysis. J. Am. Ceram. Soc., Vol. 76, p. 2707.

Murugavel, P., Kalaiselvam, M., Raju, A. R., Rao, C. N. R. 1997. Sub-micrometre spherical particles of TiO_2, ZrO_2 and PZT by nebulized spray pyrolysis of metal-organic precursor. J. Mater. Chem., Vol. 7, pp. 1433–38.

Nair, P., F. Mizukami, T. Okubo, J. Nair, K. Keizer, A. J. Burggraaf. 1997. High-temperature catalyst supports and ceramic membranes: metastability and particle packing. Ceramics processing, Vol. 43, pp. 2710–2714.

Oguri, Y., Riman, R. E., Bowen, H. K. 1988. Processing of anatase prepared from hydrothermally treated alkoxy-derived hydrous titania. J. Mater. Sci., Vol. 23, pp. 2897–2904.

Ohtani, B., Ogawa, Y., Nishimoto, S. 1997. Photocatalytic activity of amorphous-anatase mixture of titanium(IV) oxide particles suspended in aqueous solutions. J. Phys. Chem. B, Vol. 101, pp. 3746–3752.

Okuyama, K., Kousaka, Y., Tohge, N., Yamamoto, S., Wu, J. J., Flagan, R. C., Seinfeld, J. H. 1986. Production of ultrafine metal oxide aerosol particles by thermal decomposition of metal alkoxide vapors. AIChE J., Vol. 32, pp. 2010–2019.

Oliver, P. M., Watson, G. W., Kelsey, E. T., Parker, S. C. 1997. Atomistic simulation of the surface structure of the TiO_2 polymorphs rutile and anatase. J. Mater. Chem., Vol. 7, pp. 563–568.

Ollis, D. F., Pelizzetti, E., Serpone, N. 1991. Photocatalyzed destruction of water contaminants. Environ. Sci. Tech,. Vol. 25, pp. 1522–1529.

O'Regan, B., Grätzel, M. 1991. A low cost, high-efficiency solar cell based on dye-sensitized colloidal TiO_2 films. Nature, Vol. 353, pp. 737–740.

Ovenstone, J., Yanagisawa, K. 1999. Effect of hydrothermal treatment of amorphous titania on the phase change from anatase to rutile during calcination. Chem. Mater., pp. 2770–2774.

Palache, C., Berman, H., Frondel, C. 1944. The system of mineralogy. 7th ed. Vol. 1. Wiley, New York.

Park, D. G., Burlitch, J. M. 1992. Nanoparticles on anatase by electrostatic spraying of an alkoxide solution. Chem. Mater., Vol. 4, pp. 500–502.

Park, D. G., Burlitch, J. M. 1996. Electro-spray synthesis of titanium oxide nano-particles. J. Sol-Gel Sci. Tech., Vol. 6, pp. 235–249.

Parker, J. C., Siegel, R. W. 1990. Calibration of the Raman spectrum to the oxygen stoichiometry of nanophase TiO_2. Appl. Phys. Lett., Vol. 57, pp. 943–945.

Penn, R. L., Banfield, J. F. 1998. Imperfect oriented attachment: dislocation generation in defect-free nanocrystals. Science, Vol. 281, pp. 969–971.

Penn, R. L., Banfield, J. F. 1999. Formation of rutile nuclei at anatase {112} twin interfaces and the phase transformation mechanism in nanocrystalline titania. American Mineralogist, Vol. 84, pp. 871–876.

Ramamoorthy, M., Vanderbilt, D., King-Smith, R. D. 1994. First-principles calculations of the energetics of stoichiometric TiO_2 surfaces. Phys. Rev. B, Vol. 49, pp. 16723–16727.

Roberts, W. L., Campbell, T. J., Rapp, G. R. 1990. Encyclopedia of minerals. 2nd ed. Van Nostrand Reinhold, New York.

Rodriguez-Talavera, R., Vargas, S., Arroyo-Murillo, R., Montiel-Campos, R., Haro-Poniatowski, E. 1997. Modification of the phase transition temperatures in titania doped with various cations. J. Mater. Res., Vol. 12, pp. 439–443.

Rubio, J., Oteo, J. L., Villegas, M., Duran, P. 1997. Characterization and sintering behaviour of submicrometre titanium dioxide spherical particles obtained by gas-phase hydrolysis of titanium tetrabutoxide. J. Mater. Sci., Vol. 32, pp. 643–652.

Shannon, R. D., Pask, J. A. 1965. Kinetics of the anatase-rutile transformation. J. Am. Ceram. Soc., Vol. 48, pp. 391–398.

Sproson, D. W., Messing, G. L. 1987. Ceramic powder synthesis by thermal reaction of atomized solutions. In: Messing, G. L. (ed.). Advances in Ceramics. Vol. 21: Ceramic Powder Science. The American Ceramic Society, Inc., Westerville. Pp. 99–108.

Suyama, Y., Kato, A. 1976. TiO_2 produced by vapor-phase oxygenolysis of $TiCl_4$. J. Am. Ceram. Soc., 59, pp. 146–149.

Suzuki, A., Tsukuda, R. 1969. Kinetics of the transition of titanium dioxide prepared by sulfate process and chloride process. Bull. Chem. Soc. Jap., Vol. 42, pp. 1853–1857.

Vallet-Regi, M., Peña, J., Martínez, A., González-Calbet, J. M. 1993. Selection of structural type and particle size in titanium (IV) oxide. J. Mater. Res., Vol. 8, pp. 2336–2343.

Van Landuyt, J., Amelinckx, S. 1970. Shear structures in titanium oxide. Mater. Res. Bull., Vol. 5, pp. 267–274.

Visca, M., Matijevic, E. 1979. Preparation of uniform colloidal dispersions by chemical reactions in aerosols. – 1. Spherical particles of titanium dioxide. J. Coll. Interf. Sci., Vol. 68, pp. 308–319.

Wang, S. C., Flagan, R. C. 1990. Scanning electrical mobility spectrometer. Aerosol Sci. Tech., Vol. 13, pp. 230–240.

Winklmeyer, W., Reischl, G. P., Lindner, A. O., Berner, A. 1991. A new electromobility spectrometer for the measurement of aerosol size distributions in the size range from 1 to 1000 nm. J. Aerosol Sci., Vol. 22, pp. 289–296.

Xia, B. Huang,, H., Xie, Y. 1999. Heat treatment on TiO_2 nanoparticles prepared by vapor-phase hydrolysis. Mater. Sci. Eng. B, Vol. 57, pp. 150–154.

Yin, J.-S., He, L., Griffin, G. L., Ma, E. 1997. Microstructural and thermal analyses of crystallization in ultrafine amorphous titania particles. In: Ma, E., Fultz, B., Shull, R., Morral, J., Nash, P. Chemistry and physics of nanostructures and related non-equilibrium materials. The Minerals, Metals & Materials Society.

Zhang, H., Banfield, J. F. 2000a. Phase transformation of nanocrystalline anatase-to-rutile via combined interface and surface nucleation. J. Mater. Res., Vol. 15, pp. 437–448.

Zhang, H., Banfield, J. F. 2000b. Understanding polymorphic phase transformation behavior during growth of nanocrystalline aggregates: insight from TiO_2. J. Phys. Chem. B, Vol. 104, pp. 3481–3487.

Appendices of this publication are not included in the PDF version. Please order the printed version to get the complete publication (http://otatrip.hut.fi/vtt/jure/index.html

Published by

Vuorimiehentie 5, P.O.Box 2000, FIN-02044 VTT, Finland
Phone internat. +358 9 4561
Fax +358 9 456 4374

Series title, number and report code of publication

VTT Publications 439
VTT–PUBS–439

Author(s)
Ahonen, Petri

Title

Aerosol production and crystallization of titanium dioxide from metal alkoxide droplets

Abstract

In this experimental study, aerosol methods for producing titanium dioxide powders and increasing our knowledge of particle and crystal formation have been developed. Powders and ultrafine particles of titanium oxide were produced by an aerosol droplet decomposition route in tubular laminar flow reactors in air and nitrogen atmospheres. Reactor temperatures up to 1500°C were used with residence times in the range of 1–50 s. Novel methods were introduced for the production of micron sized powders, investigation of crystallization of anatase in the particles, and for studying the formation of crystal phase and morphology on ultrafine particles at different temperatures. High-resolution transmission electron microscopy, scanning electron microscopy, aerosol measurements by differential mobility analyzer and inertial impactor as well as materials characterization by diffraction and spectroscopic methods were performed. In addition, the production conditions in aerosol reactors were evaluated using computational fluid dynamics calculations. The results showed that titanium dioxide powders can be produced from ultrafine up to micron sized particles via droplet decomposition and in-droplet hydrolysis methods starting from a titanium alkoxide precursor. Crystal phase and crystallite size can be controlled by reactor conditions and by thermal post-annealing. Anatase formation in amorphous particles was observed near surfaces. Investigation of ultrafine particles revealed morphology development of rutile and anatase single crystals. The 60 and 120 nm diameter rutile crystal morphologies development was observed in mobility particle size measurements. The 20 nm diameter anatase particle morphology showed the development of crystallographic {011} and {001} surfaces.

Keywords

aerosols, particles, synthesis, pyrolysis, hydrolysis, alkoxides, titanium dioxide, anatase, rutile, crystal morphology

Activity unit

VTT Chemical Technology, Environmental Technology,
Biologinkuja 7, P.O.Box 1401, FIN–02044 VTT, Finland

ISBN			Project number
951–38–5857–X (soft back ed.) 951–38–5858–8 (URL:http://www.inf.vtt.fi/pdf/)			
Date	Language	Pages	Price
September 2001	English	55 p. + app. 62 p.	C
Name of project		Commissioned by	
		The National Technology Agency (Tekes), VTT Chemical Technology	
Series title and ISSN		Sold by	
VTT Publications 1235–0621 (soft back ed.) 1455–0849 (URL: http://www.inf.vtt.fi/pdf/)		VTT Information Service P.O.Box 2000, FIN-02044 VTT, Finland Phone internat. +358 9 456 4404 Fax +358 9 456 4374	